Understanding the anthropogenic influence on formation of biogenic secondary organic aerosols in Denmark via analysis of organosulfates and related oxidation products

Q.T. Nguyen[1,2], M.K. Christensen[1], F. Cozzi[1,*], A. Zare[1,2,3], A.M.K. Hansen[1] , K. Kristensen[1], T.E. Tulinius[1], H.H. Madsen[1], J.H. Christensen[2], J. Brandt[2], A. Massling[2], J.K. Nøjgaard[2] and M. Glasius[1]

[1] Department of Chemistry and iNANO, Aarhus University, 8000 Aarhus, Denmark

[2] Department of Environmental Science, Aarhus University, 4000 Roskilde, Denmark

[3] Institute of Geophysics, University of Tehran, Iran

* *Now at*: Department of Plant and Environmental Sciences, University of Copenhagen, 1871 Frederiksberg C, Denmark

Correspondence to: quynh@chem.au.dk

Abstract

Anthropogenic emissions of sulfur dioxide (SO_2) and nitrogen oxides (NO_x) may affect concentration levels and composition of biogenic secondary organic aerosols (BSOA) through photochemical reactions with biogenic organic precursors to form organosulfates and nitrooxy organosulfates. We investigated this influence in a field study from May 19 - June 22, 2011 at two sampling sites in Denmark. Within the study, we identified a substantial number of organic acids, organosulfates and nitrooxy organosulfates in the ambient urban curbside and semi-rural background air. A high degree of correlation in concentrations was found among a group of specific organic acids, organosulfates and nitrooxy organosulfates, which may originate from various precursors, suggesting a common mechanism or factor affecting their concentration levels at the sites. It was proposed that the formation of those species most likely occurred on a larger spatial scale with the compounds being long-range transported to the sites on the days with highest

concentrations. The origin of the long-range transported aerosols was investigated using the Hybrid Single Particle Lagrangian Integrated Trajectory (HYSPLIT) model in addition to modeled emissions of related precursors including isoprene and monoterpenes using the global Model of Emissions of Gases and Aerosols from Nature (MEGAN) and SO_2 emissions using the European Monitoring and Evaluation Program (EMEP) database. The local impacts were also studied by examining the correlation between selected species which showed significantly enhanced concentrations at the urban curbside site and the local concentrations of various gases including SO_2, ozone (O_3), NO_x, aerosol acidity and other meteorological conditions. This investigation showed that an inter-play of the local parameters such as the aerosol acidity, NO_x, SO_2, relative humidity (RH), temperature and global radiation seemed to affect the concentration level of those species, suggesting the influence of aqueous aerosol chemistry. The local impacts however seemed minor compared to the regional impacts. The total concentrations of organosulfates and nitrooxy organosulfates contributed to approximately 0.5 - 0.8 % of PM_1 mass on average at the two sampling sites.

1 Introduction

Volatile organic compounds (VOC) are emitted from both biogenic and anthropogenic sources and are oxidized to form lower volatility products partitioning between the gas and particle phase, leading to the formation of secondary organic aerosols (SOA) (Donahue et al., 2006; Kroll and Seinfeld, 2008; Jimenez et al., 2009; Hallquist et al., 2009). In general, the production of biogenic SOA (BSOA) is estimated to be significantly larger than anthropogenic SOA (ASOA) (Goldstein and Galbally, 2007; Heald et al., 2010; Spracklen et al., 2011). For example, Hallquist et al. (2009) estimated a many-fold higher annual global production of BSOA (88 TgC) compared to ASOA (10 TgC), which were however associated with high uncertainties. Other studies suggested that ASOA might have been underestimated (De Gouw and Jimenez, 2009), while some local and regional studies have indicated that ASOA could be more substantial than BSOA (Aiken et al., 2009; Fushimi et al., 2011). It is also thought that a substantial proportion of aerosols is formed through condensation of low-volatility biogenic VOC onto existing particles of anthropogenic origin (Carlton et al., 2010), thereby blurring the division between biogenic and anthropogenic SOA. Several studies have indicated that anthropogenic activities could enhance the production of BSOA via different mechanisms, for example by enhancing the incorporation of biogenic VOC products

into the condensed phase due to pre-existing organic aerosol from anthropogenic activities; affecting the SOA yield by the complex effect of the anthropogenic species NO_x and nitrate (NO_3) radical (a nighttime product of NO_2 and ozone) or affecting new particle formation and growth where sulfuric acid has been identified as having an essential role in new particle formation (Aiken et al., 2009; Carlton et al., 2010; Szidat et al., 2006; Szidat et al., 2009; Hoyle et al., 2011; Kulmala et al., 2004a). Further research is thus required on the actual impact of anthropogenic emissions on the formation and growth of SOA formed from biogenic VOC.

Several classes of VOC precursors, which are either reactive or could form oxidation products for SOA formation, have been identified. Cyclic compounds are particularly important, including compounds such as cycloalkanes, aromatic hydrocarbons, and terpenes. Terpenes are typically oxidized by an addition mechanism, yielding oxidation products with more than two polar functional groups, increasing the possibility of forming low-volatility products (Hallquist et al., 2009). A number of studies have focused on the oxidation pathways of monoterpenes by hydroxyl radical (OH), ozone (O_3) or nitrate radical (NO_3) forming organic acids such as pinonic and pinic acid as supposed first generation oxidation products (Glasius et al., 2000; Larsen et al., 2001; Yu et al., 1999; Hoffmann et al., 1997; Librando and Tringali, 2005; Surratt et al., 2008b; Calogirou et al., 1999; Yasmeen et al., 2012). The first generation products are further oxidized to form more oxidized products, for example pinonic acid is oxidized by the OH radical to form 3-methyl-1,2,3-butanetricarboxylic acid (MBTCA) (Szmigielski et al., 2007; Müller et al., 2012). Another example is the photooxidation and ozonolysis of α-pinene, one of the principal species of the monoterpene class, forming terpenylic acid and diaterpenylic acid acetate (DTAA) (Claeys et al., 2009).

Organosulfate formation has recently been demonstrated in both laboratory studies (Surratt et al., 2008b; Surratt et al., 2007a; Iinuma et al., 2007b) and ambient samples (Gómez-González et al., 2008; Kristensen and Glasius, 2011; Worton et al., 2011; Gómez-González et al., 2012) as SOA produced from the oxidation of biogenic VOC, such as isoprene, α-pinene, β-pinene and limonene in the presence of acidic sulfate particles. In addition to representing an interesting link coupling the formation of SOA from biogenic VOC precursors with the impact from anthropogenic pollutants, organosulfates were also estimated to contribute up to 5-10% of the total organic mass (Tolocka and Turpin, 2012) or even 30% of the total aerosol mass (Surratt et al., 2008b). Organosulfates and nitrooxy organosulfates are also polar compounds, which can thus enhance the ability of aerosols to act as cloud condensation nuclei (CCN) with important climate implications (Hallquist et al., 2009; IPCC, 2007).

Here we studied the occurrence, concentrations and trends of the acidic monoterpene oxidation products (including for example *cis*-pinic acid, pinonic acid, terpenylic acid, MTBCA and DTAA), oxidation products from anthropogenic VOC precursors, benzoic acid and phthalic acid (typically from aromatic hydrocarbons) or adipic acid and pimelic acid (from cyclic olefins), organosulfates, and nitrooxy organosulfates in aerosols at two different locations in Denmark. These include an urban curbside site and a semi-rural background site. The chemical analysis was performed following an approach adapted from Kristensen and Glasius (2011), employing high-performance liquid chromatography (HPLC) coupled with an electrospray ionization inlet (ESI) to a quadrupole time-of-flight mass spectrometer (q-TOF-MS). The impacts of long-range transported SOA were investigated using the Hybrid Single Particle Lagrangian Integrated Trajectory (HYSPLIT) model assisted by the modeled emissions of the major biogenic precursors including isoprene and monoterpene using the global Model of Emissions of Gases and Aerosols from Nature (MEGAN) and the anthropogenic emissions of sulfur dioxide (SO_2) using the long-range chemistry transport model, the Danish Eulerian Hemispheric Model (DEHM), based on the European Monitoring and Evaluation Program (www.EMEP.int) database. Additional support analyses were also performed, including measurement of major inorganic ions to determine the aerosol acidity level, analysis of local new particle formation events, local concentrations of atmospheric oxidants including ozone (O_3), sulfur dioxide (SO_2) and nitrogen oxides NO_x (NO_x = NO + NO_2) and other meteorological parameteres including the global radiation level, temperature, relative humidity (RH), wind direction and wind speed.

2 Experimental

2.1 Field campaign sites

The campaign was conducted during the period May 19 - June 22, 2011 concurrently at two sampling sites in Denmark (Figure 1). The sampling site HCAB (55°38′ N, 12°34' E) is located in central Copenhagen (~1.2 million inhabitants) on the curbside of H.C. Andersen's Boulevard with considerable traffic influence (~50,000 vehicles per day) (Municipality of Copenhagen, www.kk.dk). The second sampling site Risø (55°41' N, 12°05' E) is a semi-rural background site located approximately 30 km west of Copenhagen and 7 km northeast of Roskilde, which houses about 46,000 inhabitants. The semi-rural background area is characterized by agricultural land, small villages, Roskilde Fjord located about 100 m to the west of the station, and a main road (A6) located about 700 m east of the site. PM_1 samples were collected on quartz fiber filters (150 mm

diameter, Advantec QR-100) using Digitel DHA-80 High Volume Samplers (HVS) equipped with PM$_1$ sampling heads. The quartz fiber filters were pre-baked at 1000°C for 2 hours by the manufacturer to reduce organic contamination and kept in sealed bag until use. In order to assess the diurnal variation on PM$_1$ composition, sampling was performed in 12h daytime and nighttime intervals starting every day at 06:00 am and 06:00 pm local time simultaneously at both sites. The sampling flow rate was set to 23.1 m^3 h^{-1} providing a nominal sampling volume of 277.2 m^3 per 12 h sample. While this 12 h sampling interval allowed us to sample sufficient volume of the tracer compounds, the coarse time resolution complicates investigation of any short-term chemistry or transport episodes. There were several gaps in the dataset with one major gap at the Risø site from June 3 - 16 due to technical problems with the HVS. In total, 64 and 37 filter samples (including both day and night samples) were collected at HCAB and Risø, respectively. A field blank was collected in between every 12 samples or less, which showed concentrations below detection limit for the organic acids, organosulfates and nitrooxy organosulfates. The field blanks were however used for correction of concentrations of inorganic ions. The sample and blank filters were wrapped in aluminum foil and stored in anti-static bag at - 18 ^{0}C in dark condition until analysis.**2.2 Extraction**

Extraction and analysis of organic acids, organosulfates and nitrooxy organosulfates followed the procedure of Kristensen and Glasius (2011). Each filter sample (excluding a circle punch of 28 mm in diameter used for separate analysis of ions) was extracted in 75 mL of a solution consisting of 90% (v/v) acetonitrile and 10% (v/v) milli-Q water by ultra-sonication for 30 minutes in a water bath, where ice was regularly added to the bath to avoid heating. The extract was filtered through a nylon syringe filter (0.45 µm, VWR or Q-max), evaporated to dryness using a rotary evaporator and re-constituted twice in 500 µL milli-Q water containing 3% (v/v) acetonitrile and 0.1% (v/v) acetic acid. Prepared samples were kept at 3-5 °C prior to analysis. Camphoric acid was used as an internal standard to calculate the recovery. Field blanks were extracted and analyzed using the same procedure as for the samples. It has been shown that the method could sufficiently retain more volatile compounds such as pinonic acid, as well as the less volatile compounds such as pinic, terpenylic and adipic acid (Kristensen and Glasius, 2011).

2.3 HPLC-ESI-qTOF-MS analysis and quantification of compounds

Samples were analyzed using a HPLC system (Dionex Ultimate 3000) coupled through an ESI inlet to a qTOF-MS (Bruker Daltonics GmbH, Bremen, Germany). A reversed-phase HPLC separation

was achieved using a Waters Atlantis T3 C18 column (2.1 x 150 mm, 3 μm). The mobile phase was comprised of eluent A (0.1% (v/v) acetic acid in milli-Q water) and eluent B (95% (v/v) acetonitrile in milli-Q water). The injection volume was 10 μL and the flow rate of the mobile phase was 0.2 mL min^{-1} with the following gradient: the mobile phase was kept at 3% of eluent B in 10 min prior to injection until 5 min after injection; eluent B was then increased to 20% (at 20 min), 60% (at 30 min) and 95% (at 35 min) where it was kept at a plateau (95%) until 45 min and increased to 100% at 46 min; the gradient was kept at 100% of eluent B until 51 min and decreased to 3% (at 54 min) where it was further kept at 3% for 3 min. The MS scan range was set from 50 - 1000 m/z. The ESI-qTOF-MS was operated in negative ionization mode with nebulizer pressure at 3.0 bar, dry gas flow 8.0 L min^{-1}, source voltage 4000 V and transfer time 50 μs. Acquired data was processed using the Bruker Compass software.

All organic acids were quantified using authentic standards with the exception of hydroxy-pinonic acid, which was quantified using pinonic acid standard. The organosulfates and nitrooxy organosulfates were quantified using three different surrogate standards depending on the retention time of the compound. The surrogate standards included D-mannose sulfate (molecular weight = 260 g mol^{-1} (MW 260)) for compounds eluting in the first 15 min, an organosulfate from β-pinene (MW 250), which was synthesized in-house following Iinuma et al. (2009) for compounds eluting during 15 - 40 min, and octyl sulfate (MW 210) for compounds eluting after 40 min.

2.4 Extraction and analysis of ions

A circle punch (28 mm diameter) of the aerosol sample filter was sonicated in 4.00 ml milli-Q water for ½ h. The extract was filtered through a polyethersulfone syringe filter (0.45 μm, PALL Life Sciences IC Acrodisc) and analyzed by ion chromatography using a Metrohm 820 IC separation center (with a Metrosep A Supp5-150 column for anion analysis and a Metrosep C4-150 column for cation analysis) and an 819 IC conductivity detector. For anion analysis, an eluent of 3.2 mM Na$_2$CO$_3$/1.0 mM NaHCO$_3$ was used. For cation analysis, an eluent of 0.7 mM dipicolinic acid/1.7 mM HNO$_3$ was used. An auto-sampler was used where 100 μL of each sample was introduced into the eluent, which was kept at a flow rate of 0.7 mL min^{-1}. The inclusion of ion analysis in this work is mainly to calculate the level of acidity (H$^+$) from the charge balance, based on IC data of [SO$_4^{2-}$], [NO$_3^-$] and [NH$_4^+$] following Zhang et al. (2012b).

2.5 Measurement of particle number size distributions

Particle number size distributions in 15 channels from 6-700 nm were measured using a Differential Mobility Particle Sizer (DMPS), which was composed of a Vienna-type Differential Mobility Analyzer (DMA) (Winklmayer et al., 1991) employing re-circulating sheath air flow (Jokinen and Makela, 1997) and a butanol Condensation Particle Counter (CPC) (TSI Inc. 3010, Shoreview, MN). The data was corrected for reduced counting efficiency at the low size end (6-10 nm), multiply charging, and losses during sampling following inversion algorithm by Wiedensohler (1988). A ratio of sheath air to aerosol air of 6.8:1 was applied, with alternating up- and down-scans of 150s for each size spectrum. Annual service of the CPC was performed at TSI to ensure correct counting efficiency.

2.6 Biogenic VOC and SO_2 emissions

Emissions of biogenic VOCs are estimated by using the global model MEGAN (Guenther et al., 2006; Zare et al., 2013; Zare et al., 2012). The empirical algorithm in MEGAN simulates the emission rates based on relationships between ecosystem dependent emission factors and key drivers that control emissions. The model takes into account the effects of temperature, radiation, leaf area index, foliage age and soil moisture on the estimation of emissions. In MEGAN, plant species are grouped into six plant functional types (PFTs): broadleaf tree, needle leaf evergreen tree, needle leaf deciduous tree, shrub, crop and grass; and the model dataset provides the geographical distribution of the standard emission factor of the six PFTs with high spatial resolution of 1 km^2. The required meteorological inputs are provided by the MM5v3.7 model (Grell et al., 1994). The initial and boundary conditions for the MM5 model are derived from the National Center for Environmental Prediction (NCEP) FNL (Final Analyses) data with 6 h temporal and $1° × 1°$ spatial resolution (http://rda.ucar.edu/datasets/ds083.2/).

Sulfur dioxide emissions were modeled using the long-range chemistry transport model, the Danish Eulerian Hemispheric Model (DEHM) (Brandt et al., 2012), based on the European Monitoring and Evaluation Program (www.EMEP.int) database in Europe with a resolution of 50 km × 50 km. These European anthropogenic sulfur dioxide emissions are mainly released by fuel combustion (www.ceip.at), dominated by coal fired power plant and international ship traffic emissions.

2.7 Gas and meteorological data

Meteorological data including temperature, RH and global radiation were obtained from a station located on the roof-top of the H.C. Ørsted institute (HCOE, 55°42'N, 12°33'E), which represents the urban background conditions of Copenhagen, Denmark. HCOE is located ~3.5 km north of HCAB. O_3 and NO/NO_x were measured using photometry (Teledyne API 400, San Diego, CA,

1 USA), chemiluminescense (Teledyne API M200 A, San Diego, CA, USA) and infrared absorbance

2 (Teledyne API 300 E, San Diego, CA, USA), respectively at both field sites HCAB and Risø with

3 30 min resolution whereas measurement of SO_2 using UV fluorescence (Teledyne API M100E, San

4 Diego, CA, USA) with 30 min resolution was only obtained from HCAB. Gas and meteorological

5 data were collected within the Danish Air Quality Monitoring Program (Ellermann et al., 2012). As

6 nitrate radical is formed in the reaction:

7 $$NO_2 + O_3 \rightarrow NO_3 + O_2 \ (1),$$
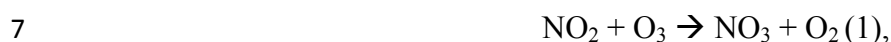
8 the production rate of NO_3 (P_{NO_3}) was determined from the measured concentrations of NO_2 and O_3

9 using equation (2):

10 $$P_{NO_3} = [NO_2][O_3]k_1 \ \text{molecule cm}^{-3}\text{s}^{-1} \ (2)$$

11 The rate constant of reaction (1) k_1 was calculated using equation (3) with available temperature

12 data:

13 $$k_1 = 1.2 \times 10^{-13} \ e^{-\frac{2450}{T}} \ \text{cm}^3\text{molecule}^{-1}\text{s}^{-1} \ (3) \ (\text{DeMore, 1997})$$

2.8 Statistical analysis

15 Statistical analysis was performed on the data set to analyze the intraday variability between

16 daytime and nighttime samples as well as the possible inter-site variation between the two sites

17 HCAB and Risø. As the data was not normally distributed, the U Mann-Whitney test was used

18 instead of a two-way ANOVA to assess the intraday and inter-site variability (Wilks, 2011).

3 Results and Discussion

3.1 Detection and characterization of organic acids, organosulfates and nitrooxy organosulfates

22 During the field campaign, a total of 39 species including 12 organic acids, 18 organosulfates (OS)

23 and 9 nitrooxy organosulfates (NOS) were detected as summarized in Table 1-3. The organic acids

24 were identified using their authentic standards, with the exception of hydroxy-pinonic acid where

25 the identification was based on the characteristic mass-to-charge (m/z) fragments of the compound.

26 The organic acids included those of anthropogenic origin (i.e. benzoic acid, adipic acid, pimelic

27 acid and phthalic acid) and biogenic origin, specifically suberic acid and azelaic acid originating

28 from unsaturated fatty acids in addition to terpenylic acid, pinonic acid, pinic acid, hydroxy-pinonic

acid, DTAA and MTBCA originating from α/β-pinene (Table 1). Among the anthropogenic organic acids, benzoic acid is a photochemical degradation product of aromatic hydrocarbons, which originate from anthropogenic automobile emissions (Suh et al., 2003), while adipic acid and pimelic acid have been identified as photooxidation products from the ozonolysis of cyclic olefins (Hatakeyama et al., 1985; Grosjean et al., 1978; Koch et al., 2000), and phthalic acid could be the oxidation product of naphthalene and other polycyclic aromatic compounds (Fine et al., 2004). The biogenic dicarboxylic acids with relatively long carbon chains including suberic acid (C_8) and azelaic acid (C_9) are believed to originate from the oxidation of unsaturated fatty acids (Mochida et al., 2003), which are common in marine phytoplankton and leaves of terrestrial higher plants, though some contribution may originate from anthropogenic meat cooking (Rogge et al., 1991) or wood burning (Rogge et al., 1998). The other biogenic organic acids (terpenylic acid, pinonic acid, pinic acid, hydroxy-pinonic acid and DTAA) are oxidation products of α/β-pinene (Claeys et al., 2009; Ma et al., 2007), with 3-methyl-1,2,3-butanetricarboxylic acid (MBTCA) being the second generation oxidation product of pinonic acid, which indicates aging by OH (Müller et al., 2012; Szmigielski et al., 2007). The identified organic acids were all detected at both sites.

The organosulfates were identified using the characteristic fragment of m/z 97 (bisulfate anion HSO_4^-) and m/z 80 (sulfur trioxide anion SO_3^-). The nitrooxy organosulfates were identified based on a neutral loss of m/z 63 (HNO_3) in addition to the characteristic fragments of HSO_4^- and SO_3^-. Many organosulfates and nitrooxy organosulfates species detected in this study (Table 2-3) have also been identified in previous smog chamber (Surratt et al., 2007a; Surratt et al., 2008b; Surratt et al., 2010) and field studies (Gómez-González et al., 2008; Kristensen and Glasius, 2011; Gómez-González et al., 2012). Most organosulfates, which were identified based on the literature probably originated from isoprene (OS molecular weight (MW) 154, 156, 170, 212, 214, 216 and 334) and monoterpenes including α- and β-pinene precursors (OS 248, 250, 280 and 298). Two organosulfates of MW 200 were identified, of which OS 200_1 could origin from isoprene via methacrylic acid epoxide (MAE) uptake onto acidified sulfate aerosol (Lin et al., 2013), while OS 200_2 could derive from 2-methyl-3-buten-2-ol (MBO) (Zhang et al., 2012b; Zhang et al., 2014). A large share of the detected nitrooxy organosulfates could be the oxidation products from limonene and/or monoterpenes (NOS 297, 311, 313, 327 and 329). The structures of several organosulfates (OS 182, OS 208, and OS 210) and one nitrooxy organosulfate (NOS 331) were not identified.

3.2 Concentrations

The ranges of concentration levels of the detected species are shown in Table 4. In general, a higher number of valid measurements (N) were available from HCAB, mostly due to the gap in the set of samples collected from the semi-rural background site Risø. The total concentrations of the detected organic acids averaged per sampling interval (12h) during the sampling period was 23 ± 15 ng m^{-3} and 19 ± 13 ng m^{-3} at HCAB and Risø, respectively, with the second generation product MBTCA accounting for approximately 21% of total organic acids at HCAB and 20% at Risø. The median value of MBTCA was 2.3 ng m^{-3} at HCAB and 2.0 ng m^{-3} at Risø, which are in range of the overall median value of 2.7 ng m^{-3} reported by Gómez-González et al. (2012) from a study at a Belgian forest site with severe urban pollution impact. Among the anthropogenic organic acids, adipic acid and phthalic acid seemed to dominate at both sites, whereas azelaic acid (4.0 ng m^{-3} average) and pinonic acid (2.2 ng m^{-3} average) were the dominant first generation biogenic organic acid at HCAB and Risø, respectively.

The organosulfates were detected in most samples from both sites (Table 4). The major organosulfates detected in high concentrations at both HCAB and Risø mostly originated from isoprene, such as OS 154, OS 156, OS 200 and OS 212 (Surratt et al., 2007a; Surratt et al., 2008b). OS 216, which was suggested to derive from the reactive uptake of isoprene epoxydiols (IEPOX) in the presence of acidic sulfate aerosol (Surratt et al., 2010; Lin et al., 2012), tends to be the most abundant organosulfate observed in prior laboratory studies and field studies in the southeastern US (Surratt et al., 2010; Lin et al., 2012; Surratt et al., 2007b; Lin et al., 2013; Surratt et al., 2008a). In this study, a moderate mean concentration of OS 216 of 5 ng m^{-3} at HCAB and 3.2 ng m^{-3} at Risø was observed. It should also be noted that we used acetonitrile as extraction solvent instead of methanol as used by Surratt et al. (2007b, 2008, 2010) and Lin et al. (2012, 2013), which could have affected the extraction yield of OS 216 in the present work. The total organosulfate concentration averaged per sampling interval (12h) during the sampling period was 60 ± 45 ng m^{-3} at HCAB, whereas at Risø a slightly lower total concentration value of 47 ± 31 ng m^{-3} was obtained. Nitrooxy organosulfates were detected in lower concentrations compared to organosulfates, with a total concentration of 4 ± 1 ng m^{-3} at HCAB and 3 ± 1 ng m^{-3} at Risø. NOS 297, which was possibly an oxidation product from limonene (Surratt et al., 2008b) was the major nitrooxy organosulfate found at both sites.

The concentration levels of the detected compounds were compared with an earlier study performed at a forest site in Denmark by Kristensen and Glasius (2011) during spring 2008, in which fewer species (six organic acids, five organosulfate, five nitrooxy organosulfates) were included. The

comparison was thus only targeted at similar compounds. In general, the concentrations of most organic acids were higher in the present study, except *cis*-pinic acid and pinonic acid, which were more abundant at the forest site. The concentration levels of the organosulfates and nitrooxy organosulfates in this study were many-fold higher compared to the previous study, especially with regards to the organosulfate species. This, in addition to the differences among the sites and years could be caused by differences in quantification standards, as Kristensen and Glasius (2011) used camphor sulfonic acid as a surrogate standard, as opposed to the three different standards including D-mannose sulfate, an in-house synthesized organosulfate from β-pinene and octyl sulfate used in this study (as described above). This highlights the analytical challenge of quantifying organosulfates and comparing concentrations among different studies.

The total concentration of organic acids and organosulfates are significantly higher in our samples compared to the Arctic, where a total concentration of 3 ± 1 ng m^{-3} for organic acids and 12 ± 2 ng m^{-3} for organosulfates (quantified using the same organosulfate from β-pinene used in the present study) were measured at Zeppelin Mountain, Svalbard during summer of 2008 (Hansen et al., 2014). However, during late winter and early spring, total concentration levels up to 70 ng m^{-3} and over 45 ng m^{-3} were detected for all organic acid, organosulfate and nitrooxy organosulfate compounds respectively at Station Nord, northeast Greenland and at Zeppelin (Hansen et al., 2014). These values are in range with our concentration values. It must be noted that a total of 11 organic acids, 12 organosulfates and one nitrooxy organosulfates were detected by Hansen et al. (2014).

3.3 Inter-site, day/night variability and inter-species correlation

The non-parametric U Mann-Whitney test was performed on the data sets to analyze the inter-site variability between HCAB and Risø during the overlapping period (May 19 - June 1 and June 17 - 22) where data from both sites were available. The 90% confidence interval was used for evaluation of the statistical significance to account for the possible field sampling, filter extraction and quantification uncertainties. The test results showed that 14 parameters out of the 41 tested parameters were statistically different between the two sites at 90% confidence interval ($p < 0.1$) (Supplementary Table 4). These 14 parameters included six organic acids (benzoic acid, pimelic acid, phtalic acid, suberic acid, pinonic acid, and azelaic acid), the concentrations of total first generation organic acids, five organosulfates (OS 182, OS 200, OS 210, OS 248 and OS 298), one nitrooxy organosulfate (NOS 297) and the concentration of total nitrooxy organosulfates. The species with statistically higher concentrations were mostly from HCAB (12 out of 14) with the

exception of benzoic acid and pinonic acid, which showed significantly higher concentrations at Risø. While a higher occurrence of benzoic acid at the semi-rural background site Risø was unexpected, it seems that the urban curbside site HCAB was associated with enhanced concentrations of both biogenic (suberic acid and azelaic acid) and anthropogenic (pimelic acid and phthalic acid) compounds in addition to the anthropogenic-biogenic coupling species (OS 182, OS 200, OS 210, OS 248, OS 298 and NOS 297), which probably indicated some local anthropogenic enhancement impacts on the concentration levels of the compounds. In fact, the total concentrations of organic acids and nitrooxy organosulfates were also found at significantly higher concentrations at HCAB. In contrast, the second generation product of pinonic acid, MBTCA, which has been regarded as an indicator of photochemical aging of pinonic acid by OH (Müller et al., 2012) was not statistically different between the two sites. The fact of a statistically higher concentration level of the pinonic acid precursor at Risø and the indifferent concentration of its product MBTCA at the sites probably suggest that the degree of photochemical aging was not directly governed by the concentrations of the precursor at the semi-rural background site Risø.

The variability between daytime and nighttime samples at each site during the whole field study was also analyzed using a non-parametric U Mann-Whitney test at 90% confidence interval. The test results showed statistically indistinguishable daytime and nighttime concentrations for most species (Supplementary Table 1-2), with the exception of higher daytime concentrations of phthalic acid ($p = 0.0385$), OS 210 ($p = 0.0622$) and NOS 343 ($p = 0.0825$) at HCAB and higher nighttime concentrations of NOS 297 at both sites ($p = 0.0011$). Phthalic acid, OS 210 and NOS 297 were associated with high numbers of valid measured daytime or nighttime concentrations ($N \geq 30$) whereas NOS 343 was associated with a lower number of valid N ($N_{day} = 10$; $N_{night} = 13$).

Phthalic acid is widely used in plasticizer substrates and could be primarily emitted to the atmosphere from off-gassing of plasticizers from plastics (Fraser et al., 2003), though previous studies have also suggested that it correlated with SOA in ambient samples (Fraser et al., 2003; Fine et al., 2004; Schauer et al., 2002). A recent study of the photooxidation of naphthalene has also indicated the link between phthalic acid formation and photochemistry, while pointing towards negligible primary emissions of the compound based on laboratory and field measurements (Kleindienst et al., 2012). The findings support our observation of higher daytime concentration of phthalic acid at HCAB, though phthalic acid was not necessarily formed directly at the site. Meanwhile the indifferent daytime and nighttime concentrations of phthalic acid at Risø were probably governed by a generally lower concentration level of the species at the site

(Supplementary Table 4). The other compound with significantly higher daytime concentrations at HCAB was OS 210, which has recently been reported in aerosols in the Arctic (Hansen et al., 2014).

The compound NOS 297 (m/z fragments 296, 233, 177, 163 and 97) showed significantly higher nighttime concentration at both sites, though its concentrations were statistically higher at HCAB compared to Risø (Supplementary Table 4). This species was previously detected in ambient aerosols (Gao et al., 2006; Reemtsma et al., 2006; Kristensen and Glasius, 2011) and has been suggested as an oxidation product of limonene-like monoterpene precursors (Surratt et al., 2008b). In this study, NOS 297 was identified as the major nitrooxy organosulfates (Table 4), accounting for 36% and 34% of the total concentrations of nitrooxy organosulfates detected at HCAB and Risø, respectively. The higher nighttime occurrence of NOS 297 could indicate the impacts of local or regional nighttime chemistry on the concentration level of the compound. In fact, the formation of nitrooxy organosulfates has been suggested to involve nighttime nitrate (NO_3) radical chemistry (Iinuma et al., 2007a; Iinuma et al., 2007b; Surratt et al., 2008b). In contrast, NOS 343 showed significantly higher daytime concentrations at HCAB, though the statistical calculation was associated with a lower number of measurements, as mentioned above. Too few measurements of NOS 343 were available at Risø to compare its daytime and nighttime concentrations. Overall, significantly higher nighttime concentrations were observed for total nitrooxy organosulfates at both sites (Supplementary Table 1-2), which was attributed to the predominant contribution from the nighttime-dominant species NOS 297. As a majority of the detected species did not show any immediate evidence of local site impacts on their concentration levels according to the U Mann-Whitney test results, the relations among the compounds were furthermore investigated using R^2 correlation coefficients to unveil any potentially driving mechanisms or factors influencing their formation. The correlation coefficients were calculated for each pair of species at each site and subsequently averaged for both sites. The averaged R^2 correlation coefficients are presented in Figure 2, with each organic acid, organosulfate and nitrooxy organosulfate compound (lines) correlating with other species (x-axis). Relative standard deviations (RSD, %) for the corresponding averaged R^2 correlation coefficient are shown in Supplementary Table 1. Only 36 out of the total 38 species were used to calculate the R^2 correlation coefficient values as those with very few measurement values were excluded. The results in Figure 2 were divided into panels of organic acids (top), organosulfates (middle) and nitrooxy organosulfates (bottom).

1   Figure 2 shows a clear correlating group with high R^2 correlation coefficient values (> 0.5) among

2   the species in the group, which is comprised of certain organic acids, organosulfates and nitrooxy

3   organosulfates. The correlating group included three organic acids, namely terpenylic acid,

4   MBTCA and DTAA (dark blue), a vast number of 12 organosulfates (red) and four nitrooxy

5   organosulfates (green). These organosulfates and nitrooxy organosulfates among others included

6   species closely related in molecular weight, such as the groups of OS (154, 156), OS (212, 214,

7   216), OS (252, 254) and NOS (327, 329, 331). The organic acids pinonic and pinic acid (light blue)

8   and OS 248 (purple) seemed to only partly follow the correlation pattern as the degree of correlation

9   was somewhat lower, especially with regards to the correlation between these species and

10 organosulfates.

11 The degree of correlation (calculated as the R^2 values) among the mentioned specific compounds

12 was persistent at both study sites, as evident by the generally lower deviation with small RSD

13 values (%) associated with averaging the R-squared values from both sites as opposed to the

14 uncorrelated species (Supplementary Table 3). The organosulfates correlated consistently well with

15 the organic acids and the other organosulfates within the correlating group, with RSD ranging from

16 typically a few to over 20% between sites. Correlation coefficients between the nitrooxy

17 organosulfates and the other species showed larger discrepancies between the two sites, with RSD

18 ranging from a few percent (NOS 313) to considerably higher percentages (NOS 327, 329 and 331),

19 mostly due to a higher correlation level of these species at Risø compared to HCAB. Concentrations

20 of pinonic acid, pinic acid and phthalic acid, which only partly followed the correlation pattern

21 showed larger deviations between the two sites. In contrast, OS 248 which also partly followed the

22 pattern (with slightly lower R^2 coefficient ~0.5) showed a highly consistent correlating tendency at

23 both sites with low RSD values. The consistent correlation pattern among the group of organic

24 acids, organosulfates and nitrooxy organosulfates of different precursors detected at both sites

25 probably indicate a common source for the species at both sites.

26 **3.4 Regional impacts**

27 Figure 3 shows the temporal variation of the total concentrations of organic acids, organosulfates,

28 nitrooxy organosulfates and PM_1 detected at HCAB and Risø during the field study. It is apparent

29 that all three classes of compounds showed similar temporal patterns, and the two sites do not differ

30 substantially, which were attributed to the large contribution of compounds belonging to the

31 correlating group affecting both sites. The observations strongly indicated that the major sources or

32 chemistry governing the total concentration levels of the compounds must occur at a spatial location

1   affecting both the urban curbside and semi-rural background sites, which represent quite different

2   environments (Figure 1). Elevated total concentrations of organic acids, organosulfates and nitrooxy

3   organosulfates seemed to occur at both sites during the same daytime or nighttime interval,

4   exemplified by the daytime samples on May 22, May 31 and June 18 or the nighttime sample on

5   May 23. Several other concentration maxima occurring on June 6 (daytime) and June 8 (nighttime)

6   were observed at HCAB (data from Risø was unavailable for these days). Organosulfate 200_2

7   (from MBO), which was mostly found at levels below the detection limit, was detected in

8   considerably higher concentrations during these episodes of concentration maxima (for example in

9   May 31, June 18 (daytime) and May 23 (nighttime) samples).

10   The correlation between the total concentration level of organosulfates and the concentration of

11   SO_4^{2-} ion measured by IC was also examined. A relatively high correlation coefficient value (R^2 =

12   0.6) was obtained between the total organosulfates and sulfate at the HCAB site with the episodes

13   of highest concentrations of organosulfates coinciding with peak concentrations of the SO_4^{2-} ion

14   (Figure 3), which is in line with previous observations of aged continental aerosols over the

15   southeast Pacific Ocean (Hawkins et al., 2010). The correlation between organosulfates and

16   inorganic sulfate also agrees with previously proposed formation mechanisms for organosulfates

17   including reactive uptake of epoxides on the surface of acidic sulfate aerosols (Iinuma et al., 2009;

18   Minerath and Elrod, 2009; Surratt et al., 2010; Lin et al., 2013; Worton et al., 2013) and sulfate

19   radical-initiated formation in the bulk phase (Nozière et al., 2010). However, while this observation

20   may support related formation processes of the organosulfates and the sulfate ion, the resemblance

21   in concentration trend among sulfate, organosulfates, organic acids, and nitrooxy organosulfates

22   may also indicate that organic acids, organosulfates and nitrooxy organosulfates could also partition

23   into existing sulfate aerosol. It should be noted that the correlation was only visible at the urban

24   curbside site HCAB, while such correlation was not found at Risø (R^2 = 0.3).

25   In general, the production rate of NO_3 radical was one order of magnitude higher at the urban site

26   HCAB compared to the semi-rural background Risø, which was also observed in an earlier study in

27   the region and attributed to higher emissions of NO_2 in urban condition (Ljungstrom and Hallquist,

28   1996). Although the formation of nitrooxy organosulfates could involve nighttime NO_3 radical

29   chemistry as discussed above, no direct correlation was found between the nighttime total

30   concentration level of nitrooxy organosulfates and the corresponding production rate of NO_3 radical

31   at HCAB (R^2 = 0.1). Meanwhile, a good correlation (R^2 = 0.6) of nighttime P_{NO_3} and nighttime total

32   concentration of nitrooxy organosulfates was found at Risø (Figure 3). The difference could be

1   attributed to the continuous emissions of NO from automobiles in the city centre, which reacts with

2   NO_3 radical and complicates the observed trend of its production rate.

3   $$NO_3 + NO \rightarrow 2NO_2 \ (4)$$

4   In addition, the observed concentrations of nitrooxy organosulfates could also be affected by both

5   local and long-range transported impacts. The extent and impact of long-range transport, the impact

6   of the interplay between O_3, NO_2 and the production rate of NO_3 radical on the possible local

7   species will be discussed in more detail below.

8   In order to investigate the regional impacts on the concentration levels of the detected compounds,

9   5-days air mass back trajectories were calculated using the Hybrid Single Particle Lagrangian

10   Integrated Trajectory (HYSPLIT) model for every 12h sample (Draxier and Hess, 1998). As HCAB

11   and Risø are relatively close with a distance of ~30 km, HYSPLIT calculations were only

12   performed for the HCAB site. The results revealed a dominating westerly origin of air masses

13   during most of the campaign period. However a clear dominance of the south-easterly air masses

14   was found to be associated with the daytime or nighttime episodes of elevated concentrations,

15   including the daytime samples on May 22, 26 and 31 and June 6 and 18 and the nighttime sample

16   on June 8. The travelling path of the south-easterly air masses probably involved the region around

17   the borders between Germany, Poland and Czech Republic (Figure 1, 4). It must be noted that the

18   air masses following the south-easterly direction could have different origins (3-5 days backwards)

19   but all passed the south-easterly region 1-2 days immediately before arrival at the sampling site. An

20   example of the impacts of air masses arriving from the south-easterly direction is shown for three

21   consecutive days on May 30th (nighttime), May 31 (daytime with elevated concentrations) and June

22   1 (daytime) where data from both HCAB and Risø were available (Figure 4). To support the

23   interpretation of the HYSPLIT calculations, emissions of isoprene and monoterpenes (daily)

24   calculated using the MEGAN model and SO_2 (monthly) calculated using the DEHM model, are also

25   shown in Figure 4 to illustrate the magnitude of biogenic and anthropogenic emissions in the

26   region.

27   Figure 4 shows a sudden change of air mass origin from westerly (May 30) to south-easterly (May

28   31) back to westerly (June 1), which was coupled with a major episode on May 31 with elevated

29   concentrations of the organic acids, organosulfates and nitrooxy organosulfates (Figure 3). The

30   modeled isoprene and monoterpene daily emissions did not vary noticeably over the corresponding

31   days (Figure 4), while emissions from the westerly direction affecting May 30 and June 1 seemed

1 comparable to emissions from the southeasterly direction affecting May 31. This indicated that

2 VOC emissions were probably not the limiting factor in the formation of the investigated

3 compounds.

4 Figure 4 also shows a map of average SO_2 emission over the two months May - June 2011. Though

5 the SO_2 emission map could not be used to evaluate the daily change in anthropogenic emissions to

6 further investigate the observed elevated concentrations on May 31, it however indicated strong SO_2

7 emissions from hotspots in the region that were passed over by the south-easterly air mass shown in

8 the trajectories. This could probably influence the formation of the organosulfates and nitrooxy

9 organosulfates during long-range transport to the sites. The accompanying organic acids, which

10 were also found at high concentrations correlating to the organosulfates and nitrooxy

11 organosulfates, could also be long-range transported to the sampling sites.

12 It is difficult to determine the exact spatial location of the major sources or chemistry governing the

13 total concentrations of the compounds at the two sites, which is partly due to the coarse resolution

14 of the SO_2 emission map. However, it is unlikely that the major source location would be in the

15 local proximity of the two sites due to the highly different local conditions between the urban

16 curbside site HCAB and the semi-rural background site Risø (Figure 1). Such a local source, if

17 present, would be subject to immediate different local background conditions and also varying local

18 wind conditions, while in contrast, a highly similar temporal variation pattern of total observed

19 concentrations was found at the sites during the whole campaign period (Figure 3). Furthermore,

20 any possible point source located southeasterly from HCAB and Risø, which could affect both

21 sampling sites would unlikely be in Denmark, as both sites are located only 10 - 20 km from Baltic

22 sea in the southeasterly direction (Figure 1). The source region therefore is possibly located at the

23 broader regional scale across the Baltic sea extending to the southerly neighboring countries.

24 Particle mass concentrations were calculated based on integration of the calculated particle mass

25 size distributions (from DMPS data), which were further based on measured particle number size

26 distributions assuming particle sphericity, using a SOA particle density of 1.7 g cm^{-3} (Stock et al.,

27 2011) (Figure 3). This density value is close to the bulk densities of ammonium sulfate and nitrate,

28 which are expected to be the major components of aged accumulation mode particles. The detected

29 and quantified organosulfates and nitrooxy organosulfates contributed to 0.1 - 1.0 % (approximately

30 0.5 % on average) of PM_1 mass at HCAB and 0.4 - 1.5 % (approximately 0.8 % on average) of PM_1

31 mass at Risø. The values are considerably lower than previous estimates, including 30% (Surratt et

al., 2008b) or 5-10% contribution of organosulfates to total organic mass (Tolocka and Turpin, 2012). PM_1 concentrations at HCAB were in the lower range during the days under the influence of southeasterly air mass (May 22, May 26, May 31, June 18 (daytime), with the exception of June 6 (daytime). The period of high PM_1 concentrations at HCAB (June 6 - 8) seemed to link to other local conditions, including episodes of elevated concentrations of SO_2 and NO_x (Figure 5 and Supplementary Figure 1). The local impacts are further discussed in the section below.

3.5 Local impacts

The possible local anthropogenic impacts were investigated by examining the species of significantly higher concentrations at HCAB, which did not belong to the correlating group, including OS 182 (m/z fragments 181, 97), OS 210 (m/z fragments 209, 153, 137, 97 and 79) and NOS 297 (m/z fragments 233, 177, 163 and 97). As displayed in Figure 5, the patterns of changes in OS 182 and OS 210 concentrations in May were considerably similar, with a few episodes of high daytime concentrations especially during the period May 20 - 25 with a lower concentration on May 22 (daytime). Such observation stands in contrast to the trend of the total organosulfate concentrations during the same period, where a generally lower concentration level was observed except from elevated daytime concentrations on May 22 (Figure 3). Assuming that the trend of variations the total detected species in Figure 3 was mostly governed by long-range transported compounds belonging to the highly correlated group, the trend of OS 182 and OS 210, which did not belong to the correlated group, could probably reflect some local impact on the concentration levels of these species. However, while OS 182 and OS 210 seemed to correlate well in May, concentrations of the species deviated towards the end of the field study (Figure 5), which could be partly attributed to additional input from long-range transport to the site. For example, elevated daytime concentration of OS 182 was observed on June 16, which is one of the characteristic days of southeasterly arriving air masses associated with higher total concentrations of the detected species (Figure 3).

Local impacts were studied to explain the significantly higher concentrations of OS 182, OS 210 and NOS 297 at the urban curbside site HCAB. Temporal variation of gases (NO, NO_x and SO_2), aerosol acidity level (calculated from charge balance using $[SO_4^{2-}]$, $[NO_3^-]$, and $[NH_4^+]$ following Zhang et al. (2012b)) at HCAB (Figure 5), and meteorological conditions including RH (Figure 5), temperature (Temp) and global radiation (GR) (Supplementary Figure 1) at the urban background site HCOE, which was located in close proximity to HCAB were analyzed. As can be seen from Figure 5, the period May 20 - 25 was accompanied by a generally higher level of aerosol acidity

which decreased on May 22 (daytime). Such variation of the aerosol acidity level perfectly matched the trend of the varying concentrations of OS 210 and OS 182 during the same period (Figure 5). In fact, the aerosol acidity level has been suggested as an essential parameter in the formation of organosulfates (Zhang et al., 2012b). At the same time, the concentration level of the organosulfates might rather be affected by an inter-play between the aerosol acidity level and other factors, such as the global radiation and temperature. For example the May 20 and 21 (daytime) samples showed high concentrations of OS 182 and OS 210, which was comparable to the concentrations on May 24 or 25 (daytime) samples (Figure 5), whereas the aerosol acidity level on May 20 or 21 was considerably lower on May 20 and 21 (daytime) compared to the other days (Figure 6). May 20 - 21 were however accompanied with a higher level of global radiation, especially on May 21 (579 W m^{-2}) compared to other latter days May 24-25 (daytime) (Supplementary Figure 1). While a higher level of global radiation could probably enhance the oxidation of SO_2 by the OH radical and thereby resulted in higher concentrations of SO_4^{2-} as observed with the May 20 - 21 (daytime) samples, NH_4^+ was also detected at higher concentrations with these samples, resulting in an overall lower aerosol acidity calculated based on ion charge balance on the days. In addition, the higher temperature observed on May 20 - 21 compared to May 24 - 25 may also have contributed to enhance the formation of supposed local organosulfates in the former samples, by means of enhancing biogenic VOC emissions, or photochemistry in general. In fact, a considerably higher level of O_3 oxidant was also found during the former days (May 20 - 21) compared to the latter days (May 24 - 25), which would positively enhance the formation of SOA.

Higher daytime concentrations of OS 210 were also observed on June 7 and 8 , whereas the aerosol acidity reached its highest level of 46 nmol m^{-3} on June 7 (nighttime) with interestingly almost neutral conditions on the adjacent June 7 (daytime) and June 8 (daytime) (Figure 5). At the same time, during these two daytime intervals, higher average concentrations of SO_2 were also observed. At the same time, concentrations of NO and NO_x in higher resolution (30 min) were also considerably elevated (Supplementary Figure 1). . Meanwhile, the O_3 level was in the lowest concentration range presumably due to the lower level of sunlight in addition to titration by NO_x (figure not shown). A close examination revealed that the NO and NO_x were highest during the early morning and late afternoon hours which are attributed to traffic emissions, though during the day course both NO and NO_x remained at a higher level compared to the other days during the campaign period. This observation could be partially attributed to lower wind speed during daytime on June 7 (2.0 m s^{-1}) and on June 8 (2.9 m s^{-1}), which was considerably lower than the average wind

speed of 4.1 m s^{-1} for the whole campaign period. It must also be noted that this period was coupled with the highest RH range during the campaign period (Supplementary Figure 2), which resulted from the corresponding very low global radiation during the days. The observations indicated an inter-play between the anthropogenic gases, especially NO, NO$_x$ and probably aqueous aerosol chemistry, leading to the occurrence of higher concentrations of OS 210 in these samples. A previous study by Dommen et al. (2006) on the effect of RH under high NO$_x$ conditions indicated that more volatile SOA were observed at higher RH rather than at lower RH. Additionally, SOA formation including carboxylic acids and organosulfur compounds in cloud and fog droplets have been hypothesized as plausible by Blando and Turpin (2000) while a recent smog chamber study by Zhang et al. (2012a) suggested that elevated RH values could mediate the formation of organosulfates, thereby emphasizing the role of wet sulfate aerosols in forming organosulfates in ambient aerosols. At the same time, though aerosol acidity has been found to enhance isoprene SOA formation under low initial NO conditions (Surratt et al., 2010; Surratt et al., 2007c; Jaoui et al., 2010), seed aerosol acidity showed a negligible effect on SOA formation from isoprene under high initial NO conditions (Surratt et al., 2006), which implied the less important role of seed aerosol acidity on the formation of OS 210 on June 7 and 8 (daytime) where both NO and RH were high.

Further investigation of the meteorological conditions during the period where data from both sites were available (May 19 - June 1 and June 17 - June 22, see Supplementary Figure 2) revealed a possible coupling between higher temperature and global radiation (508 Wm^{-2}) with the occurrence of concentration maxima observed on days with the highest temperature May 31 (daytime) and June 6 (daytime) (Figure 3). However, information was lacking on the spatial scale of high temperature and global radiation episodes to fully justify if concentration maxima were enhanced by high temperature and global radiation at source or at the sampling sites.

The third species used to study the local impacts was NOS 297, which showed significantly higher nighttime concentration as discussed above. A recent work by Rollins et al. (2013) has also suggested a correlation between nitrooxy organosulfates, including NOS 297 and total particulate organic nitrate (RONO$_2$), which results from oxidation of organic compounds in high NO$_x$ environment and NO$_3$ radical chemistry. Although some possible long-range transport contribution to the observed concentration of NOS 297 at HCAB could not be completely eliminated, as shown by its elevated concentration seen during peak concentration days May 31 and June 16, elevated concentrations of NOS 297 were observed predominantly at nighttime on May 19, 20, 22, 26 and

June 6, 8 and 10. To examine the local impacts on NOS 297, only nighttime production rate of NO_3 radical and nighttime RH are shown (Figure 5). The RH condition during the nights of high concentrations of NOS 297 covered both the lower RH range (May 19, May 20 and June 10) and the higher RH range (May 22, June 6 and June 8) of the whole campaign. Very high production rate of NO_3 radical (12.8 and 9.7 x 10^7 molecule cm^{-3} s^{-1}, respectively) was observed during the nights of highest RH, June 6 and 8, whereas during the in-between night June 7, when RH was still in the high range, lower P_{NO_3} was observed, which was coupled with considerably lower concentration of NOS 297. In contrast, lower P_{NO_3} was also observed during other nights of higher NOS 297 concentrations with lower RH condition (May 19, 20 and June 10). However, a lower RH range could also reduce the available condensation sink for particle precursors and thus facilitate the formation of NOS 297 by nighttime NO_3 radical chemistry. It is thus unlikely if any single parameter such as RH or P_{NO_3} could be a prerequisite for the occurrence of elevated concentration of NOS 297 in this study. In addition, investigation of air mass back trajectories using HYSPLIT also revealed that the May 22, 26 and June 6 nighttime were affected by air masses arriving from the south-south-easterly direction whereas on June 8 air masses arrived from easterly direction. Such observations suggest that the detected nighttime concentrations of NOS 297 could be governed by both the local formation and the degree of long-range transport of the compound to the site. As a result, no direct correlation between nighttime concentrations of NOS 297 and P_{NO_3} was observed ($R^2 = 0.2$). On the other hand, it should be noted that during this period of the year, the duration of the night is relatively short in Denmark, therefore calculation of nighttime concentrations would couple with higher uncertainty. Nevertheless, it seems probable that occurrence of NOS 297 was favored by nighttime chemistry, regardless of whether the species were formed in-situ or long-range transported to the site.

Local new particle formation (NPF) events were also examined using the DMPS data following Dal Maso et al. (2005) to investigate whether the local formation of organosulfates could be associated with particle nucleation at the sites. A limited number of NPF events were found occurring on the same days at the semi-rural background site Risø, the urban background site HCOE and the urban curbside site HCAB, though HCAB is heavily influenced by traffic emissions resulting in generally short nucleation bursts rather than allowing a classic "banana" formation and growth. The NPFs however seemed to occur on the days with low concentrations of most organic acid, organosulfate and nitrooxy organosulfate species, including the possible local compounds OS 182 and OS 210,

which agree with previous indications that NPF may occur more frequently in cleaner environments (Lyubovtseva et al., 2005; Kulmala et al., 2004b). As the occurrence of higher concentrations of the detected organic acids, organosulfates and nitrooxy organosulfates did not correspond to NPF events, which were coupled with elevated occurrence of smaller-sized particles; it is likely that the organic acids, organosulfates and nitrooxy organosulfates belong to the accumulation mode. At the same time, any correlation to NPF should be investigated with size-segregated samples.

4 Conclusion

A field study was conducted from May 19 to June 22, 2011 at two sites in Denmark, including the urban curbside site HCAB and the semi-rural background site Risø to investigate the anthropogenic impacts on the formation of biogenic SOA via analysis of organosulfates and related oxidation products using HPLC-qTOF-MS. A substantial range of anthropogenic and biogenic organic acids, organosulfates and nitrooxy organosulfates were detected, identified and quantified. Isoprene oxidation products comprised a large fraction of the detected organosulfates whereas a majority of the detected nitrooxy organosulfates may originate from limonene and/or monoterpenes. The U Mann-Whitney statistical test showed significantly higher concentrations of specific biogenic and anthropogenic species at HCAB, whereas an intraday statistical test only revealed significantly higher daytime concentrations of phthalic acid and OS 210 and significantly higher nighttime concentrations of NOS 297. Many detected compounds including a group of organic acids, organosulfates and nitrooxy organosulfates of various precursors were found belonging to a common highly correlated group, consistently affecting their concentration levels at both sites, suggesting a common source region or similarities in formation processes. The analysis of HYSPLIT back trajectories together with isoprene and monoterpene emissions calculated by the MEGAN model and SO_2 emission based on the EMEP monitoring database indicated that south-easterly air mass arriving from across the Baltic sea could relate to the corresponding episodes of the elevated total concentrations at the sites, implying the importance of the regional impacts on the occurrence of the compounds.

The local impacts were also investigated for several selected species which showed significantly higher concentrations at HCAB compared to Risø and did not belong to the correlating group, including OS 182, OS 210 and NOS 297. The results showed that the local factors including aerosol acidity, RH, NO and probably some wet aerosol chemistry could possibly lead to a higher occurrence of the organosulfates, whereas the major nitrooxy organosulfate NOS 297 could be

favoured by nighttime chemistry, in addition to temperature and global radiation, which could also enhance the concentrations of the long-range transported species at the sites. As only very few compounds were deemed as affected by the local conditions, the analysis of the local impacts was restricted to a modest number of compounds. In general, the regional impacts seemed to considerably exceed the local impacts. It was estimated that organosulfates and nitrooxy organosulfates contributed to approximately 0.5% and 0.8% of PM_1 mass, respectively at HCAB and Risø.

Acknowledgements

References

Aiken, A. C., Salcedo, D., Cubison, M. J., Huffman, J. A., DeCarlo, P. F., Ulbrich, I. M., Docherty, K. S., Sueper, D., Kimmel, J. R., Worsnop, D. R., Trimborn, A., Northway, M., Stone, E. A., Schauer, J. J., Volkamer, R. M., Fortner, E., de Foy, B., Wang, J., Laskin, A., Shutthanandan, V., Zheng, J., Zhang, R., Gaffney, J., Marley, N. A., Paredes-Miranda, G., Arnott, W. P., Molina, L. T., Sosa, G., and Jimenez, J. L.: Mexico City aerosol analysis during MILAGRO using high resolution aerosol mass spectrometry at the urban supersite (T0) - Part 1: Fine particle composition and organic source apportionment, Atmos Chem Phys, 9, 6633-6653, 2009.

Blando, J. D., and Turpin, B. J.: Secondary organic aerosol formation in cloud and fog droplets: a literature evaluation of plausibility, Atmos Environ, 34, 1623-1632, Doi 10.1016/S1352-2310(99)00392-1, 2000.

Brandt, J., Silver, J. D., Frohn, L. M., Geels, C., Gross, A., Hansen, A. B., Hansen, K. M., Hedegaard, G. B., Skjoth, C. A., Villadsen, H., Zare, A., and Christensen, J. H.: An integrated model study for Europe and North America using the Danish Eulerian Hemispheric Model with focus on intercontinental transport of air pollution, Atmos Environ, 53, 156-176, DOI 10.1016/j.atmosenv.2012.01.011, 2012.

Calogirou, A., Larsen, B. R., and Kotzias, D.: Gas-phase terpene oxidation products: a review, Atmos Environ, 33, 1423-1439, Doi 10.1016/S1352-2310(98)00277-5, 1999.

Carlton, A. G., Pinder, R. W., Bhave, P. V., and Pouliot, G. A.: To What Extent Can Biogenic SOA be Controlled?, Environ Sci Technol, 44, 3376-3380, Doi 10.1021/Es903506b, 2010.

Claeys, M., Iinuma, Y., Szmigielski, R., Surratt, J. D., Blockhuys, F., Van Alsenoy, C., Boge, O., Sierau, B., Gomez-Gonzalez, Y., Vermeylen, R., Van der Veken, P., Shahgholi, M., Chan, A. W. H., Herrmann, H., Seinfeld, J. H., and Maenhaut, W.: Terpenylic Acid and Related Compounds from the Oxidation of alpha-Pinene: Implications for New Particle Formation and Growth above Forests, Environ Sci Technol, 43, 6976-6982, Doi 10.1021/Es9007596, 2009.

Dal Maso, M., Kulmala, M., Riipinen, I., Wagner, R., Hussein, T., Aalto, P. P., and Lehtinen, K. E. J.: Formation and growth of fresh atmospheric aerosols: eight years of aerosol size distribution data from SMEAR II, Hyytiala, Finland, Boreal Environment Research, 10, 323-336, 2005.

De Gouw, J., and Jimenez, J. L.: Organic Aerosols in the Earth's Atmosphere, Environ Sci Technol, 43, 7614-7618, Doi 10.1021/Es9006004, 2009.

DeMore, W. B., Sander, S.P., Golden, D.M., Hampson, R.F., Kurylo, M.J. Howard, C.J., Ravishankara, A.R., Kolb, C.E., Molina, M.J.: Chemical Kinetics and Photochemical Data for use in Stratospheric Modeling, Evaluation No. 12,, NASA Panel for Data Evaluation, Jet Propulsion Laboratory Publication 97-4, Pasadena, CA, January 15. http://jpldataeval.jpl.nasa.gov/pdf/Atmos97_Anotated.pdf, 1997.

Dommen, J., Metzger, A., Duplissy, J., Kalberer, M., Alfarra, M. R., Gascho, A., Weingartner, E., Prevot, A. S. H., Verheggen, B., and Baltensperger, U.: Laboratory observation of oligomers in the aerosol from isoprene/NO(x) photooxidation, Geophysical Research Letters, 33, Doi 10.1029/2006gl026523, 2006.

Donahue, N. M., Robinson, A. L., Stanier, C. O., and Pandis, S. N.: Coupled partitioning, dilution, and chemical aging of semivolatile organics, Environ Sci Technol, 40, 2635-2643, Doi 10.1021/Es052297c, 2006.

Draxier, R. R., and Hess, G. D.: An overview of the HYSPLIT_4 modelling system for trajectories, dispersion and deposition, Aust Meteorol Mag, 47, 295-308, 1998.

Ellermann, T., Nøjgaard, J. K., Nordstrøm, C., Brandt, J., Christensen, J., Ketzel, M., and Jensen, S. S.: The Danish Air Quality Monitoring Programme. Annual Summary for 2011. , Scientific Report from DCE - Danish Centre for Environment and Energy No. 37. 63 pp. http://www2.dmu.dk/Pub/SR37.pdf, 2012.

Fine, P. M., Chakrabarti, B., Krudysz, M., Schauer, J. J., and Sioutas, C.: Diurnal variations of individual organic compound constituents of ultrafine and accumulation mode particulate matter in the Los Angeles basin, Environ Sci Technol, 38, 1296-1304, 10.1021/Es0348389, 2004.

Fraser, M. P., Cass, G. R., and Simoneit, B. R. T.: Air quality model evaluation data for organics. 6. C-3-C-24 organic acids, Environ Sci Technol, 37, 446-453, 10.1021/Es0209262, 2003.

Fushimi, A., Wagai, R., Uchida, M., Hasegawa, S., Takahashi, K., Kondo, M., Hirabayashi, M., Morino, Y., Shibata, Y., Ohara, T., Kobayashi, S., and Tanabe, K.: Radiocarbon (C-14) Diurnal Variations in Fine Particles at Sites Downwind from Tokyo, Japan in Summer, Environ Sci Technol, 45, 6784-6792, Doi 10.1021/Es201400p, 2011.

Galloway, M. M., Chhabra, P. S., Chan, A. W. H., Surratt, J. D., Flagan, R. C., Seinfeld, J. H., and Keutsch, F. N.: Glyoxal uptake on ammonium sulphate seed aerosol: reaction products and reversibility of uptake under dark and irradiated conditions, Atmos Chem Phys, 9, 3331-3345, 2009.

Gao, S., Surratt, J. D., Knipping, E. M., Edgerton, E. S., Shahgholi, M., and Seinfeld, J. H.: Characterization of polar organic components in fine aerosols in the southeastern United States: Identity, origin, and evolution, J Geophys Res-Atmos, 111, Doi 10.1029/2005jd006601, 2006.

Glasius, M., Lahaniati, M., Calogirou, A., Di Bella, D., Jensen, N. R., Hjorth, J., Kotzias, D., and Larsen, B. R.: Carboxylic acids in secondary aerosols from oxidation of cyclic monoterpenes by ozone, Environ Sci Technol, 34, 1001-1010, Doi 10.1021/Es990445r, 2000.

Goldstein, A. H., and Galbally, I. E.: Known and unexplored organic constituents in the Earth's atmosphere, Environ Sci Technol, 41, 1514-1521, 2007.

Gómez-González, Y., Surratt, J. D., Cuyckens, F., Szmigielski, R., Vermeylen, R., Jaoui, M., Lewandowski, M., Offenberg, J. H., Kleindienst, T. E., Edney, E. O., Blockhuys, F., Van Alsenoy, C., Maenhaut, W., and Claeys, M.: Characterization of organosulfates from the photooxidation of isoprene and unsaturated fatty acids in ambient aerosol using liquid chromatography/(-) electrospray ionization mass spectrometry, Journal of Mass Spectrometry, 43, 371-382, Doi 10.1002/Jms.1329, 2008.

Gómez-González, Y., Wang, W., Vermeylen, R., Chi, X., Neirynck, J., Janssens, I. A., Maenhaut, W., and Claeys, M.: Chemical characterisation of atmospheric aerosols during a 2007 summer field campaign at Brasschaat, Belgium: sources and source processes of biogenic secondary organic aerosol, Atmos Chem Phys, 12, 125-138, DOI 10.5194/acp-12-125-2012, 2012.

Grell, G. A., Dudhia, J., and Stauffer, D. R.: A description of the fifth-generation Penn State/NCAR mesoscale model (MM5), NCAR/TN-398 STR, Penn State/NCAR, 1994.

Grosjean, D., Vancauwenberghe, K., Schmid, J. P., Kelley, P. E., and Pitts, J. N.: Identification of C3-C10 Aliphatic Dicarboxylic-Acids in Airborne Particulate Matter, Environ Sci Technol, 12, 313-317, Doi 10.1021/Es60139a005, 1978.

Guenther, A., Karl, T., Harley, P., Wiedinmyer, C., Palmer, P. I., and Geron, C.: Estimates of global terrestrial isoprene emissions using MEGAN (Model of Emissions of Gases and Aerosols from Nature), Atmos Chem Phys, 6, 3181-3210, 2006.

Hallquist, M., Wenger, J. C., Baltensperger, U., Rudich, Y., Simpson, D., Claeys, M., Dommen, J., Donahue, N. M., George, C., Goldstein, A. H., Hamilton, J. F., Herrmann, H., Hoffmann, T., Iinuma, Y., Jang, M., Jenkin, M. E., Jimenez, J. L., Kiendler-Scharr, A., Maenhaut, W., McFiggans, G., Mentel, T. F., Monod, A., Prevot, A. S. H., Seinfeld, J. H., Surratt, J. D., Szmigielski, R., and Wildt, J.: The formation, properties and impact of secondary organic aerosol: current and emerging issues, Atmos Chem Phys, 9, 5155-5236, 2009.

Hansen, A. M. K., Kristensen, K., Nguyen, Q. T., Zare, A., Cozzi, F., Nøjgaard, J. K., Skov, H., Brandt, J., Christensen, J. H., Ström, J., Tunved, P., Krejci, R., and Glasius, M.: Organosulfates and organic acids in Arctic aerosols: speciation, annual variation and concentration levels, Atmos. Chem. Phys. Discuss., 14, 4745-4785, 10.5194/acpd-14-4745-2014, 2014.

Hatakeyama, S., Tanonaka, T., Weng, J. H., Bandow, H., Takagi, H., and Akimoto, H.: Ozone Cyclohexene Reaction in Air - Quantitative-Analysis of Particulate Products and the Reaction-Mechanism, Environ Sci Technol, 19, 935-942, Doi 10.1021/Es00140a008, 1985.

Hawkins, L. N., Russell, L. M., Covert, D. S., Quinn, P. K., and Bates, T. S.: Carboxylic acids, sulfates, and organosulfates in processed continental organic aerosol over the southeast Pacific

Ocean during VOCALS-REx 2008, J Geophys Res-Atmos, 115, D13201 Doi 10.1029/2009jd013276, 2010.

Heald, C. L., Kroll, J. H., Jimenez, J. L., Docherty, K. S., DeCarlo, P. F., Aiken, A. C., Chen, Q., Martin, S. T., Farmer, D. K., and Artaxo, P.: A simplified description of the evolution of organic aerosol composition in the atmosphere, Geophysical Research Letters, 37, Doi 10.1029/2010gl042737, 2010.

Hoffmann, T., Odum, J. R., Bowman, F., Collins, D., Klockow, D., Flagan, R. C., and Seinfeld, J. H.: Formation of organic aerosols from the oxidation of biogenic hydrocarbons, Journal of Atmospheric Chemistry, 26, 189-222, 1997.

Hoyle, C. R., Boy, M., Donahue, N. M., Fry, J. L., Glasius, M., Guenther, A., Hallar, A. G., Hartz, K. H., Petters, M. D., Petaja, T., Rosenoern, T., and Sullivan, A. P.: A review of the anthropogenic influence on biogenic secondary organic aerosol, Atmos Chem Phys, 11, 321-343, DOI 10.5194/acp-11-321-2011, 2011.

Iinuma, Y., Muller, C., Berndt, T., Boge, O., Claeys, M., and Herrmann, H.: Evidence for the existence of organosulfates from beta-pinene ozonolysis in ambient secondary organic aerosol, Environ Sci Technol, 41, 6678-6683, Doi 10.1021/Es070938t, 2007a.

Iinuma, Y., Muller, C., Boge, O., Gnauk, T., and Herrmann, H.: The formation of organic sulfate esters in the limonene ozonolysis secondary organic aerosol (SOA) under acidic conditions, Atmos Environ, 41, 5571-5583, DOI 10.1016/j.atmosenv.2007.03.007, 2007b.

Iinuma, Y., Boge, O., Kahnt, A., and Herrmann, H.: Laboratory chamber studies on the formation of organosulfates from reactive uptake of monoterpene oxides, Phys Chem Chem Phys, 11, 7985-7997, Doi 10.1039/B904025k, 2009.

IPCC: Summary for Policymakers. In: Climate Change 2007: The Physical Science Basis. Contribution of Working Group I to the Fourth Assessment Report of the Intergovernmental Panel on Climate Change [Solomon, S., D. Qin, M. Manning, Z. Chen, M. Marquis, K.B. Averyt, M. Tignor and H.L. Miller (eds.)]. Cambridge University Press, Cambridge, United Kingdom and New York, NY, USA., 2007.

Jaoui, M., Corse, E. W., Lewandowski, M., Offenberg, J. H., Kleindienst, T. E., and Edney, E. O.: Formation of organic tracers for isoprene SOA under acidic conditions, Atmos Environ, 44, 1798-1805, DOI 10.1016/j.atmosenv.2010.01.018, 2010.

Jimenez, J. L., Canagaratna, M. R., Donahue, N. M., Prevot, A. S. H., Zhang, Q., Kroll, J. H., DeCarlo, P. F., Allan, J. D., Coe, H., Ng, N. L., Aiken, A. C., Docherty, K. S., Ulbrich, I. M., Grieshop, A. P., Robinson, A. L., Duplissy, J., Smith, J. D., Wilson, K. R., Lanz, V. A., Hueglin, C., Sun, Y. L., Tian, J., Laaksonen, A., Raatikainen, T., Rautiainen, J., Vaattovaara, P., Ehn, M., Kulmala, M., Tomlinson, J. M., Collins, D. R., Cubison, M. J., Dunlea, E. J., Huffman, J. A., Onasch, T. B., Alfarra, M. R., Williams, P. I., Bower, K., Kondo, Y., Schneider, J., Drewnick, F., Borrmann, S., Weimer, S., Demerjian, K., Salcedo, D., Cottrell, L., Griffin, R., Takami, A., Miyoshi, T., Hatakeyama, S., Shimono, A., Sun, J. Y., Zhang, Y. M., Dzepina, K., Kimmel, J. R., Sueper, D., Jayne, J. T., Herndon, S. C., Trimborn, A. M., Williams, L. R., Wood, E. C.,

1 Middlebrook, A. M., Kolb, C. E., Baltensperger, U., and Worsnop, D. R.: Evolution of Organic
2 Aerosols in the Atmosphere, Science, 326, 1525-1529, DOI 10.1126/science.1180353, 2009.

3 Jokinen, V., and Makela, J. M.: Closed-loop arrangement with critical orifice for DMA sheath
4 excess flow system, Journal of Aerosol Science, 28, 643-648, 1997.

5 Kleindienst, T. E., Jaoui, M., Lewandowski, M., Offenberg, J. H., and Docherty, K. S.: The
6 formation of SOA and chemical tracer compounds from the photooxidation of naphthalene and its
7 methyl analogs in the presence and absence of nitrogen oxides, Atmos Chem Phys, 12, 8711-8726,
8 DOI 10.5194/acp-12-8711-2012, 2012.

9 Koch, S., Winterhalter, R., Uherek, E., Kolloff, A., Neeb, P., and Moortgat, G. K.: Formation of
10 new particles in the gas-phase ozonolysis of monoterpenes, Atmos Environ, 34, 4031-4042, Doi
11 10.1016/S1352-2310(00)00133-3, 2000.

12 Kristensen, K., and Glasius, M.: Organosulfates and oxidation products from biogenic
13 hydrocarbons in fine aerosols from a forest in North West Europe during spring, Atmos Environ,
14 45, 4546-4556, DOI 10.1016/j.atmosenv.2011.05.063, 2011.

15 Kroll, J. H., and Seinfeld, J. H.: Chemistry of secondary organic aerosol: Formation and evolution
16 of low-volatility organics in the atmosphere, Atmos Environ, 42, 3593-3624, DOI
17 10.1016/j.atmosenv.2008.01.003, 2008.

18 Kulmala, M., Laakso, L., Lehtinen, K. E. J., Riipinen, I., Dal Maso, M., Anttila, T., Kerminen, V.
19 M., Horrak, U., Vana, M., and Tammet, H.: Initial steps of aerosol growth, Atmos Chem Phys, 4,
20 2553-2560, 2004a.

21 Kulmala, M., Vehkamaki, H., Petaja, T., Dal Maso, M., Lauri, A., Kerminen, V. M., Birmili, W.,
22 and McMurry, P. H.: Formation and growth rates of ultrafine atmospheric particles: a review of
23 observations, Journal of Aerosol Science, 35, 143-176, DOI 10.1016/j.jaerosci.2003.10.003, 2004b.

24 Larsen, B. R., Di Bella, D., Glasius, M., Winterhalter, R., Jensen, N. R., and Hjorth, J.: Gas-phase
25 OH oxidation of monoterpenes: Gaseous and particulate products, Journal of Atmospheric
26 Chemistry, 38, 231-276, Doi 10.1023/A:1006487530903, 2001.

27 Librando, V., and Tringali, G.: Atmospheric fate of OH initiated oxidation of terpenes. Reaction
28 mechanism of alpha-pinene degradation and secondary organic aerosol formation, Journal of
29 Environmental Management, 75, 275-282, DOI 10.1016/j.jenvman.2005.01.001, 2005.

30 Lin, Y. H., Zhang, Z. F., Docherty, K. S., Zhang, H. F., Budisulistiorini, S. H., Rubitschun, C. L.,
31 Shaw, S. L., Knipping, E. M., Edgerton, E. S., Kleindienst, T. E., Gold, A., and Surratt, J. D.:
32 Isoprene Epoxydiols as Precursors to Secondary Organic Aerosol Formation: Acid-Catalyzed
33 Reactive Uptake Studies with Authentic Compounds, Environ Sci Technol, 46, 250-258, Doi
34 10.1021/Es202554c, 2012.

35 Lin, Y. H., Zhang, H. F., Pye, H. O. T., Zhang, Z. F., Marth, W. J., Park, S., Arashiro, M., Cui, T.
36 Q., Budisulistiorini, H., Sexton, K. G., Vizuete, W., Xie, Y., Luecken, D. J., Piletic, I. R., Edney, E.
37 O., Bartolotti, L. J., Gold, A., and Surratt, J. D.: Epoxide as a precursor to secondary organic
38 aerosol formation from isoprene photooxidation in the presence of nitrogen oxides, P Natl Acad Sci
39 USA, 110, 6718-6723, DOI 10.1073/pnas.1221150110, 2013.

Ljungstrom, E., and Hallquist, M.: Nitrate radical formation rates in Scandinavia, Atmos Environ, 30, 2925-2932, Doi 10.1016/1352-2310(96)00006-4, 1996.

Lyubovtseva, Y. S., Sogacheva, L., Dal Maso, M., Bonn, B., Keronen, P., and Kulmala, M.: Seasonal variations of trace gases, meteorological parameters, and formation of aerosols in boreal forests, Boreal Environment Research, 10, 493-510, 2005.

Ma, Y., Willcox, T. R., Russell, A. T., and Marston, G.: Pinic and pinonic acid formation in the reaction of ozone with alpha-pinene, Chemical Communications, 1328-1330, Doi 10.1039/B.617130c, 2007.

Minerath, E. C., and Elrod, M. J.: Assessing the Potential for Diol and Hydroxy Sulfate Ester Formation from the Reaction of Epoxides in Tropospheric Aerosols, Environ Sci Technol, 43, 1386-1392, Doi 10.1021/Es8029076, 2009.

Mochida, M., Kawabata, A., Kawamura, K., Hatsushika, H., and Yamazaki, K.: Seasonal variation and origins of dicarboxylic acids in the marine atmosphere over the western North Pacific, J Geophys Res-Atmos, 108, Doi 10.1029/2002jd002355, 2003.

Müller, L., Reinnig, M. C., Naumann, K. H., Saathoff, H., Mentel, T. F., Donahue, N. M., and Hoffmann, T.: Formation of 3-methyl-1,2,3-butanetricarboxylic acid via gas phase oxidation of pinonic acid - a mass spectrometric study of SOA aging, Atmos Chem Phys, 12, 1483-1496, DOI 10.5194/acp-12-1483-2012, 2012.

Nozière, B., Ekström, S., Alsberg, T., and Holmström, S.: Radical-initiated formation of organosulfates and surfactants in atmospheric aerosols, Geophysical Research Letters, 37, L05806, 10.1029/2009GL041683, 2010.

Reemtsma, T., These, A., Venkatachari, P., Xia, X., Hopke, P. K., Springer, A., and Linscheid, M.: Identification of Fulvic Acids and Sulfated and Nitrated Analogues in Atmospheric Aerosol by Electrospray Ionization Fourier Transform Ion Cyclotron Resonance Mass Spectrometry, Analytical Chemistry, 78, 8299-8304, 10.1021/ac061320p, 2006.

Rogge, W. F., Hildemann, L. M., Mazurek, M. A., Cass, G. R., and Simonelt, B. R. T.: Sources of Fine Organic Aerosol .1. Charbroilers and Meat Cooking Operations, Environ Sci Technol, 25, 1112-1125, Doi 10.1021/Es00018a015, 1991.

Rogge, W. F., Hildemann, L. M., Mazurek, M. A., Cass, G. R., and Simoneit, B. R. T.: Sources of fine organic aerosol. 9. Pine, oak and synthetic log combustion in residential fireplaces, Environ Sci Technol, 32, 13-22, Doi 10.1021/Es960930b, 1998.

Schauer, J. J., Fraser, M. P., Cass, G. R., and Simoneit, B. R. T.: Source reconciliation of atmospheric gas-phase and particle-phase pollutants during a severe photochemical smog episode, Environ Sci Technol, 36, 3806-3814, Doi 10.1021/Es011458j, 2002.

Spracklen, D. V., Jimenez, J. L., Carslaw, K. S., Worsnop, D. R., Evans, M. J., Mann, G. W., Zhang, Q., Canagaratna, M. R., Allan, J., Coe, H., McFiggans, G., Rap, A., and Forster, P.: Aerosol mass spectrometer constraint on the global secondary organic aerosol budget, Atmos Chem Phys, 11, 12109-12136, DOI 10.5194/acp-11-12109-2011, 2011.

Stock, M., Cheng, Y. F., Birmili, W., Massling, A., Wehner, B., Müller, T., Leinert, S., Kalivitis, N., Mihalopoulos, N., and Wiedensohler, A.: Hygroscopic properties of atmospheric aerosol particles over the Eastern Mediterranean: implications for regional direct radiative forcing under clean and polluted conditions, Atmos. Chem. Phys., 11, 4251-4271, 10.5194/acp-11-4251-2011, 2011.

Suh, I., Zhang, R. Y., Molina, L. T., and Molina, M. J.: Oxidation mechanism of aromatic peroxy and bicyclic radicals from OH-toluene reactions, Journal of the American Chemical Society, 125, 12655-12665, Doi 10.1021/Ja0350280, 2003.

Surratt, J. D., Murphy, S. M., Kroll, J. H., Ng, N. L., Hildebrandt, L., Sorooshian, A., Szmigielski, R., Vermeylen, R., Maenhaut, W., Claeys, M., Flagan, R. C., and Seinfeld, J. H.: Chemical composition of secondary organic aerosol formed from the photooxidation of isoprene, Journal of Physical Chemistry A, 110, 9665-9690, Doi 10.1021/Jp061734m, 2006.

Surratt, J. D., Kroll, J. H., Kleindienst, T. E., Edney, E. O., Claeys, M., Sorooshian, A., Ng, N. L., Offenberg, J. H., Lewandowski, M., Jaoui, M., Flagan, R. C., and Seinfeld, J. H.: Evidence for organosulfates in secondary organic aerosol, Environ Sci Technol, 41, 517-527, 2007a.

Surratt, J. D., Lewandowski, M., Offenberg, J. H., Jaoui, M., Kleindienst, T. E., Edney, E. O., and Seinfeld, J. H.: Effect of acidity on secondary organic aerosol formation from isoprene, Environ Sci Technol, 41, 5363-5369, 2007b.

Surratt, J. D., Lewandowski, M., Offenberg, J. H., Jaoui, M., Kleindienst, T. E., Edney, E. O., and Seinfeld, J. H.: Effect of acidity on secondary organic aerosol formation from isoprene, Environ Sci Technol, 41, 5363-5369, Doi 10.1021/Es0704176, 2007c.

Surratt, J. D., Gomez-Gonzalez, Y., Chan, A. W., Vermeylen, R., Shahgholi, M., Kleindienst, T. E., Edney, E. O., Offenberg, J. H., Lewandowski, M., Jaoui, M., Maenhaut, W., Claeys, M., Flagan, R. C., and Seinfeld, J. H.: Organosulfate formation in biogenic secondary organic aerosol, J Phys Chem A, 112, 8345-8378, 10.1021/jp802310p, 2008a.

Surratt, J. D., Gomez-Gonzalez, Y., Chan, A. W. H., Vermeylen, R., Shahgholi, M., Kleindienst, T. E., Edney, E. O., Offenberg, J. H., Lewandowski, M., Jaoui, M., Maenhaut, W., Claeys, M., Flagan, R. C., and Seinfeld, J. H.: Organosulfate formation in biogenic secondary organic aerosol, Journal of Physical Chemistry A, 112, 8345-8378, Doi 10.1021/Jp802310p, 2008b.

Surratt, J. D., Chan, A. W., Eddingsaas, N. C., Chan, M., Loza, C. L., Kwan, A. J., Hersey, S. P., Flagan, R. C., Wennberg, P. O., and Seinfeld, J. H.: Reactive intermediates revealed in secondary organic aerosol formation from isoprene, Proc Natl Acad Sci U S A, 107, 6640-6645, 10.1073/pnas.0911114107, 2010.

Szidat, S., Jenk, T. M., Synal, H. A., Kalberer, M., Wacker, L., Hajdas, I., Kasper-Giebl, A., and Baltensperger, U.: Contributions of fossil fuel, biomass-burning, and biogenic emissions to carbonaceous aerosols in Zurich as traced by C-14, J Geophys Res-Atmos, 111, Doi 10.1029/2005jd006590, 2006.

Szidat, S., Ruff, M., Perron, N., Wacker, L., Synal, H. A., Hallquist, M., Shannigrahi, A. S., Yttri, K. E., Dye, C., and Simpson, D.: Fossil and non-fossil sources of organic carbon (OC) and

elemental carbon (EC) in Goteborg, Sweden, Atmos Chem Phys, 9, 1521-1535, DOI 10.5194/acp-9-1805-2009, 2009.

Szmigielski, R., Surratt, J. D., Gomez-Gonzalez, Y., Van der Veken, P., Kourtchev, I., Vermeylen, R., Blockhuys, F., Jaoui, M., Kleindienst, T. E., Lewandowski, M., Offenberg, J. H., Edney, E. O., Seinfeld, J. H., Maenhaut, W., and Claeys, M.: 3-methyl-1,2,3-butanetricarboxylic acid: An atmospheric tracer for terpene secondary organic aerosol, Geophysical Research Letters, 34, Doi 10.1029/2007gl031338, 2007.

Tolocka, M. P., and Turpin, B.: Contribution of Organosulfur Compounds to Organic Aerosol Mass, Environ Sci Technol, 46, 7978-7983, 10.1021/Es300651v, 2012.

Wiedensohler, A.: An Approximation of the Bipolar Charge-Distribution for Particles in the Sub-Micron Size Range, Journal of Aerosol Science, 19, 387-389, 1988.

Wilks, D. S.: Statistical methods in the atmospheric sciences, 3rd ed., International geophysics series, 100, Elsevier/Academic Press, Amsterdam ; Boston, xix, 676 p. pp., 2011.

Winklmayer, W., Reischl, G. P., Lindner, A. O., and Berner, A.: New electromobility spectrometer for the measurement of aerosol size distributions in the size range 1 to 1000 nm, Journal of Aerosol Science, 22, 289-296, 1991.

Worton, D. R., Goldstein, A. H., Farmer, D. K., Docherty, K. S., Jimenez, J. L., Gilman, J. B., Kuster, W. C., de Gouw, J., Williams, B. J., Kreisberg, N. M., Hering, S. V., Bench, G., McKay, M., Kristensen, K., Glasius, M., Surratt, J. D., and Seinfeld, J. H.: Origins and composition of fine atmospheric carbonaceous aerosol in the Sierra Nevada Mountains, California, Atmos Chem Phys, 11, 10219-10241, DOI 10.5194/acp-11-10219-2011, 2011.

Worton, D. R., Surratt, J. D., LaFranchi, B. W., Chan, A. W. H., Zhao, Y. L., Weber, R. J., Park, J. H., Gilman, J. B., de Gouw, J., Park, C., Schade, G., Beaver, M., St Clair, J. M., Crounse, J., Wennberg, P., Wolfe, G. M., Harrold, S., Thornton, J. A., Farmer, D. K., Docherty, K. S., Cubison, M. J., Jimenez, J. L., Frossard, A. A., Russell, L. M., Kristensen, K., Glasius, M., Mao, J. Q., Ren, X. R., Brune, W., Browne, E. C., Pusede, S. E., Cohen, R. C., Seinfeld, J. H., and Goldsteint, A. H.: Observational Insights into Aerosol Formation from Isoprene, Environ Sci Technol, 47, 11403-11413, Doi 10.1021/Es4011064, 2013.

Yasmeen, F., Vermeylen, R., Maurin, N., Perraudin, E., Doussin, J. F., and Claeys, M.: Characterisation of tracers for aging of alpha-pinene secondary organic aerosol using liquid chromatography/negative ion electrospray ionisation mass spectrometry, Environmental Chemistry, 9, 236-246, Doi 10.1071/En11148, 2012.

Yu, J. Z., Cocker, D. R., Griffin, R. J., Flagan, R. C., and Seinfeld, J. H.: Gas-phase ozone oxidation of monoterpenes: Gaseous and particulate products, Journal of Atmospheric Chemistry, 34, 207-258, Doi 10.1023/A:1006254930583, 1999.

Zare, A., Christensen, J. H., Irannejad, P., and Brandt, J.: Evaluation of two isoprene emission models for use in a long-range air pollution model, Atmos Chem Phys, 12, 7399-7412, DOI 10.5194/acp-12-7399-2012, 2012.

1   Zare, A., Christensen, J. H., Gross, A., Irannejad, P., Glasius, M., and Brandt, J.: Quantifying the
2   contributions of natural emissions to ozone and total fine PM concentrations in the Northern
3   Hemisphere, Atmos. Chem. Phys. Discuss., 13, 16775-16830, 10.5194/acpd-13-16775-2013, 2013.

4   Zhang, H., Zhang, Z., Cui, T., Lin, Y.-H., Bhathela, N. A., Ortega, J., Worton, D. R., Goldstein, A.
5   H., Guenther, A., Jimenez, J. L., Gold, A., and Surratt, J. D.: Secondary Organic Aerosol Formation
6   via 2-Methyl-3-buten-2-ol Photooxidation: Evidence of Acid-Catalyzed Reactive Uptake of
7   Epoxides, Environmental Science & Technology Letters, 1, 242-247, 10.1021/ez500055f, 2014.

8   Zhang, H. F., Lin, Y. H., Zhang, Z. F., Zhang, X. L., Shaw, S. L., Knipping, E. M., Weber, R. J.,
9   Gold, A., Kamens, R. M., and Surratt, J. D.: Secondary organic aerosol formation from
10   methacrolein photooxidation: roles of NOx level, relative humidity and aerosol acidity,
11   Environmental Chemistry, 9, 247-262, Doi 10.1071/En12004, 2012a.

12   Zhang, H. F., Worton, D. R., Lewandowski, M., Ortega, J., Rubitschun, C. L., Park, J. H.,
13   Kristensen, K., Campuzano-Jost, P., Day, D. A., Jimenez, J. L., Jaoui, M., Offenberg, J. H.,
14   Kleindienst, T. E., Gilman, J., Kuster, W. C., de Gouw, J., Park, C., Schade, G. W., Frossard, A. A.,
15   Russell, L., Kaser, L., Jud, W., Hansel, A., Capellin, L., Karl, T., Glasius, M., Guenther, A.,
16   Goldstein, A. H., Seinfeld, J. H., Gold, A., Kamens, R. M., and Surratt, J. D.: Organosulfates as
17   Tracers for Secondary Organic Aerosol (SOA) Formation from 2-Methyl-3-Buten-2-ol (MBO) in
18   the Atmosphere, Environ Sci Technol, 46, 9437-9446, Doi 10.1021/Es301648z, 2012b.

19   Zhang, H. F., Worton, D. R., Lewandowski, M., Ortega, J., Rubitschun, C. L., Park, J. H.,
20   Kristensen, K., Campuzano-Jost, P., Day, D. A., Jimenez, J. L., Jaoui, M., Offenberg, J. H.,
21   Kleindienst, T. E., Gilman, J., Kuster, W. C., de Gouw, J., Park, C., Schade, G. W., Frossard, A. A.,
22   Russell, L., Kaser, L., Jud, W., Hansel, A., Cappellin, L., Karl, T., Glasius, M., Guenther, A.,
23   Goldstein, A. H., Seinfeld, J. H., Gold, A., Kamens, R. M., and Surratt, J. D.: Organosulfates as
24   Tracers for Secondary Organic Aerosol (SOA) Formation from 2-Methyl-3-Buten-2-ol (MBO) in
25   the Atmosphere, Environ Sci Technol, 46, 9437-9446, Doi 10.1021/Es301648z, 2012c.

26

27

28

List of Tables

Supplementary Information

Supplementary Table 1. Statistical results of U Mann-Whitney test performed on daytime and nighttime concentrations of the organic acids, organosulfates and nitrooxy organosulfate detected at HCAB. Statistically different parameters (with p-level < 0.1) are underlined. Parameters with two few measurements (N < 5) were excluded from the test.

Supplementary Table 2. Statistical results of U Mann-Whitney test performed on daytime and nighttime concentrations of the organic acids, organosulfates and nitrooxy organosulfate detected at Risø. Statistically different parameters (with p-level < 0.1) are underlined. Parameters with two few measurements (N < 5) were excluded from the test.

Supplementary Table 3. Relative standard deviations (RSD, %), which were associated with averaging R-square correlation coefficients (between pairs of compounds) at the two sites, were calculated. The species belonging or partly belonging to a common correlating group are marked in blue shade with the corresponding RSD in red (those only partly belonging to the group underlined). RSD values seemed low for the correlating organic acids and OS while larger for the NOS, mostly due to higher correlation coefficients at Risø. The partly-correlating species pinic, pinonic acid and phthalic acid showed relatively larger RSD compared to the other correlating compounds, while another partly-correlating species (OS 248) showed a consistent partly correlating degree at both sites as evident by small RSD values.

Supplementary Table 4. Statistical results of U Mann-Whitney test performed on the organic acids, organosulfates and nitrooxy organosulfate detected at the two sampling sites H.C. Andersen Boulevard (HCAB) and Risø. 14 out of 41 tested parameters are statistically different with p-level < 0.1 (underlined).

Supplementary Figure 1. Temporal variation of concentration of selected gases SO$_2$, NO, and NO$_x$ (30 min resolution) at HCAB during the campaign period. The x-axis shows a temporal scale from 00 - 24h for each day, with the white and grey shades indicating the intervals for day and night samples, respectively.

Supplementary Figure 2. Temporal variation (30 min resolution) of the local meteorological parameters at the urban background site HCOE, including relative humidity (RH), global radiation (GR) and temperature (T). The x-axis shows a temporal scale from 00 - 24h for each day, with the white and grey shades indicating the intervals for day and night samples, respectively.

Figures

Figure 1. Locations of the urban curbside station H.C. Andersen Boulevard (HCAB) and the semi-rural background station (Risø) (map.krak.dk and map.google.dk). HCAB is located in the city centre of Copenhagen close nearby a busy street. Risø is located approximately 30 km west of HCAB.

1 Figure 2. Correlations between organic acids, organosulfates and nitrooxy organosulfates with each

2 other detected species in each sample throughout the sampling period (excluding those with too few

3 measurements), expressed as correlation coefficient (R^2). The results show R^2 coefficient averaged

4 from the two sites. High R^2 values (> 0.5) were found among a specific group of species (yellow

5 shade), suggesting common sources. A few other species including pinonic acid, pinic acid, phthalic

6 acid, and OS 248 also partly followed the correlation pattern.

7

8

9
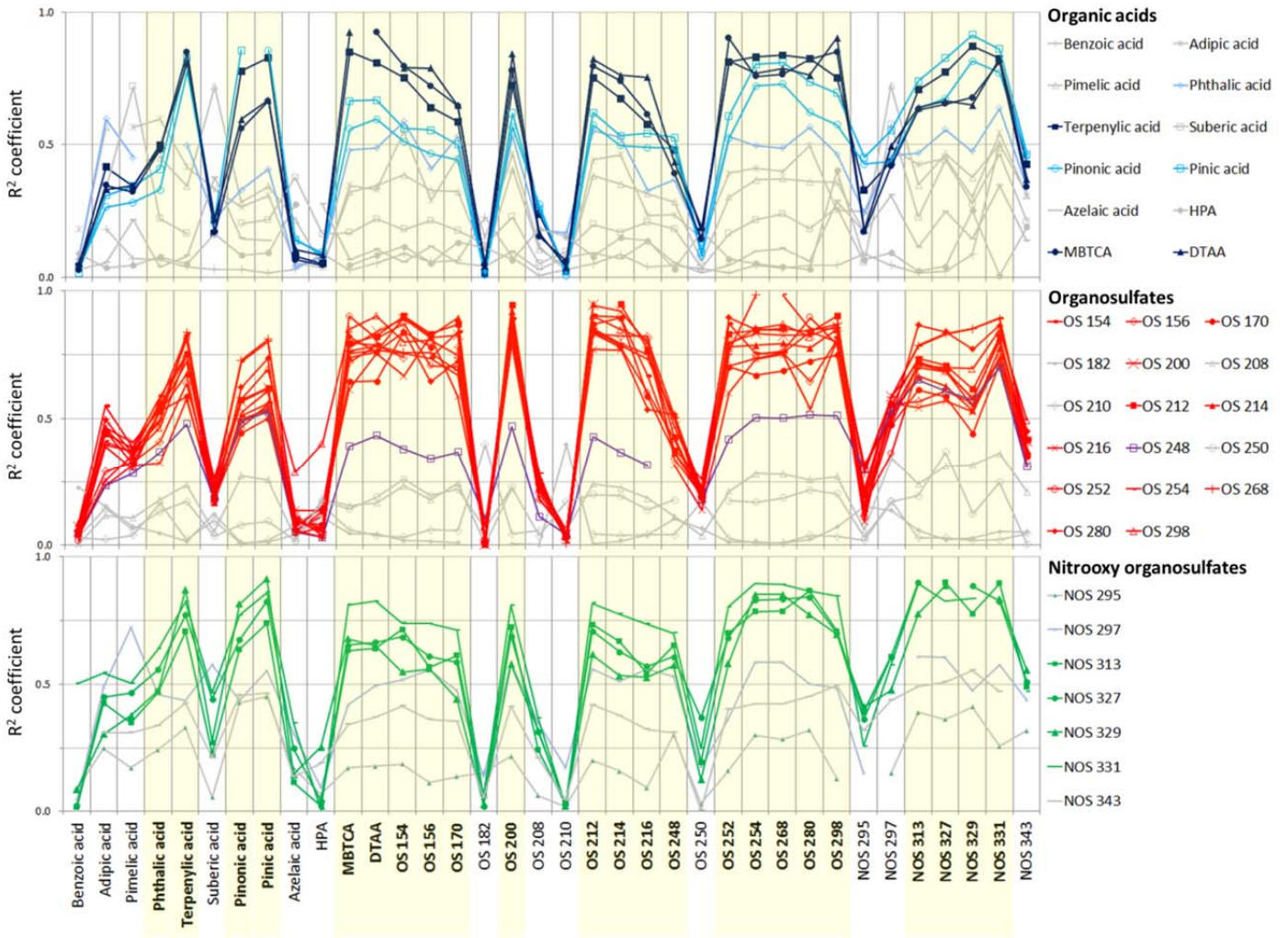
Figure 3. Temporal trends of total concentrations of organic acids, organosulfates and nitrooxy organosulfates at the urban curbside site HCAB (solid line) and the semi-rural background site Risø (broken line). The figure shows a strong correlation between the two sites and among the three categories of compounds examined. Sulfate (HCAB) and production rate of NO_3 radical (Risø) are also shown in the organosulfate and nitrooxy organosulfate panels, respectively.
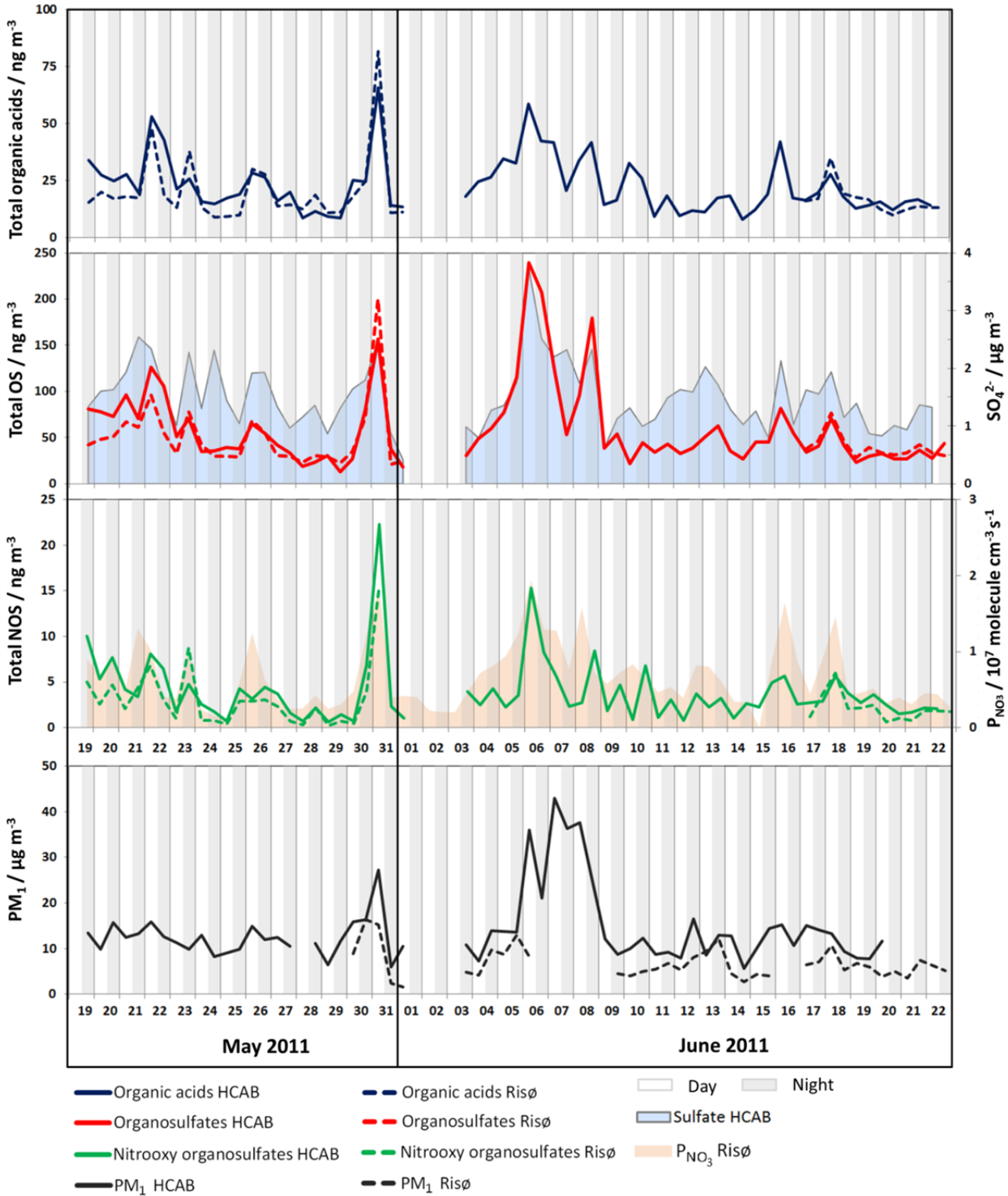
Figure 4. A sudden change in air mass back trajectories on May 31 to southeasterly direction was coupled with elevated concentrations of organosulfates, nitrooxy organosulfates, and organic acids at both HCAB and Risø. Modeled daily isoprene and monoterpene emissions did not vary significantly over the three days. The SO_2 emission map (May-June average) showed a higher abundance of emission hotspots in southeasterly direction (observed on May 31) compared to the westerly direction (observed on May 30 and June 1). HCAB is marked at the bottom tip of the black triangle.
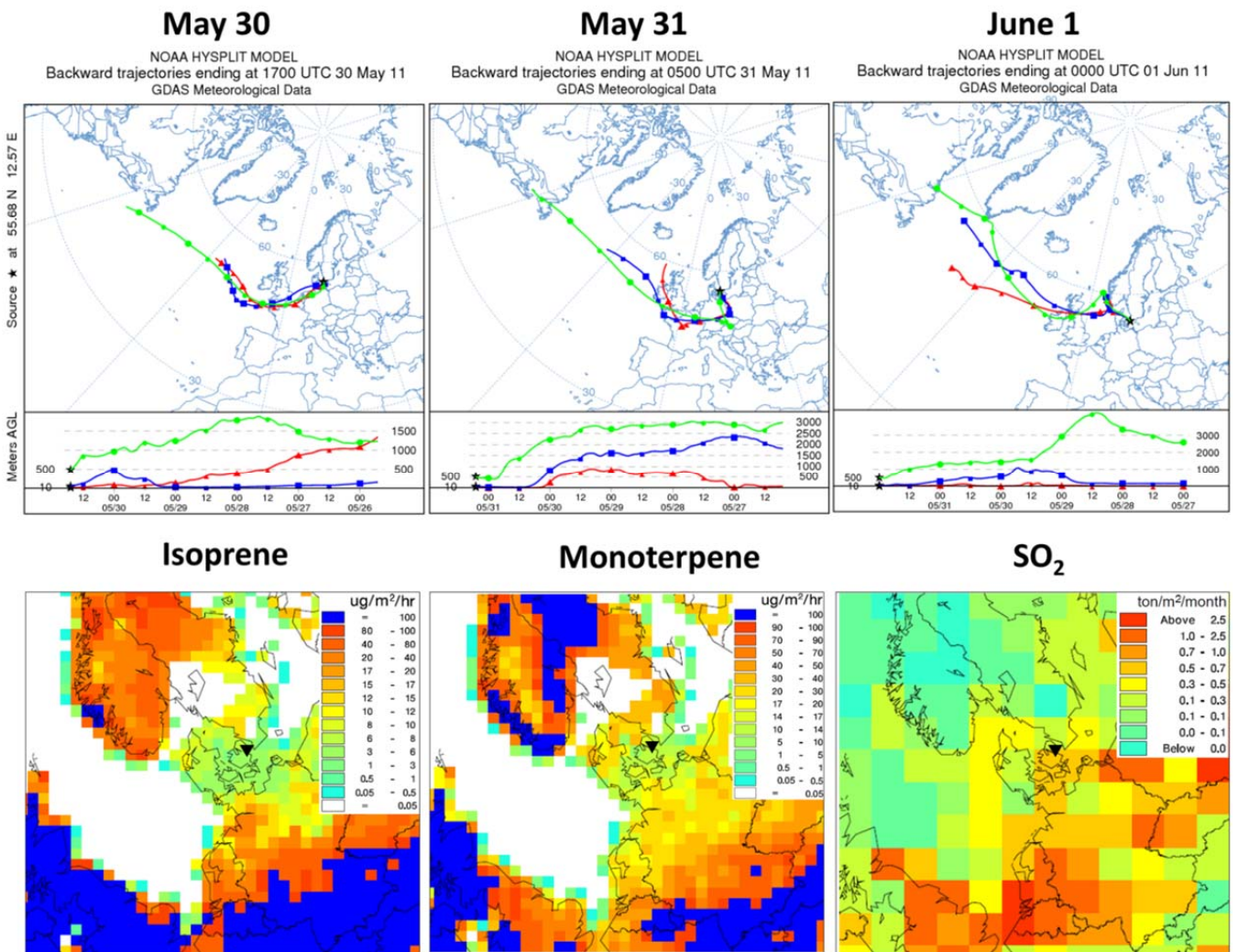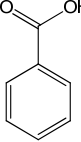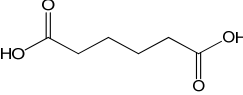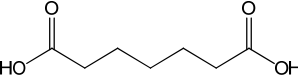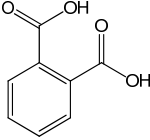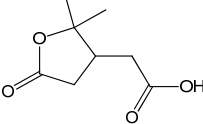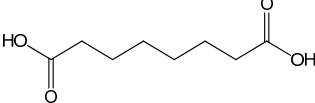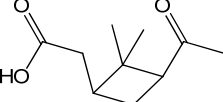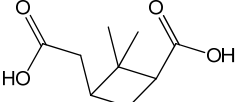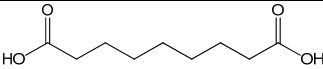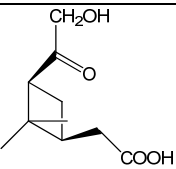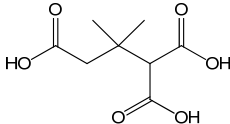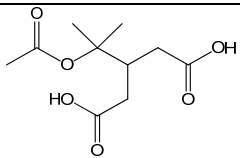
Figure 5. Time profiles of selected species of significantly higher concentration levels at HCAB, including OS 182, OS 210 and NOS 297. Concentrations of OS 182 and OS 210 are shown against level of SO_2 and acidity at HCAB, while concentration trend of NOS 297 is shown against nighttime production rate of NO_3 radical and nighttime relative humidity at HCAB.
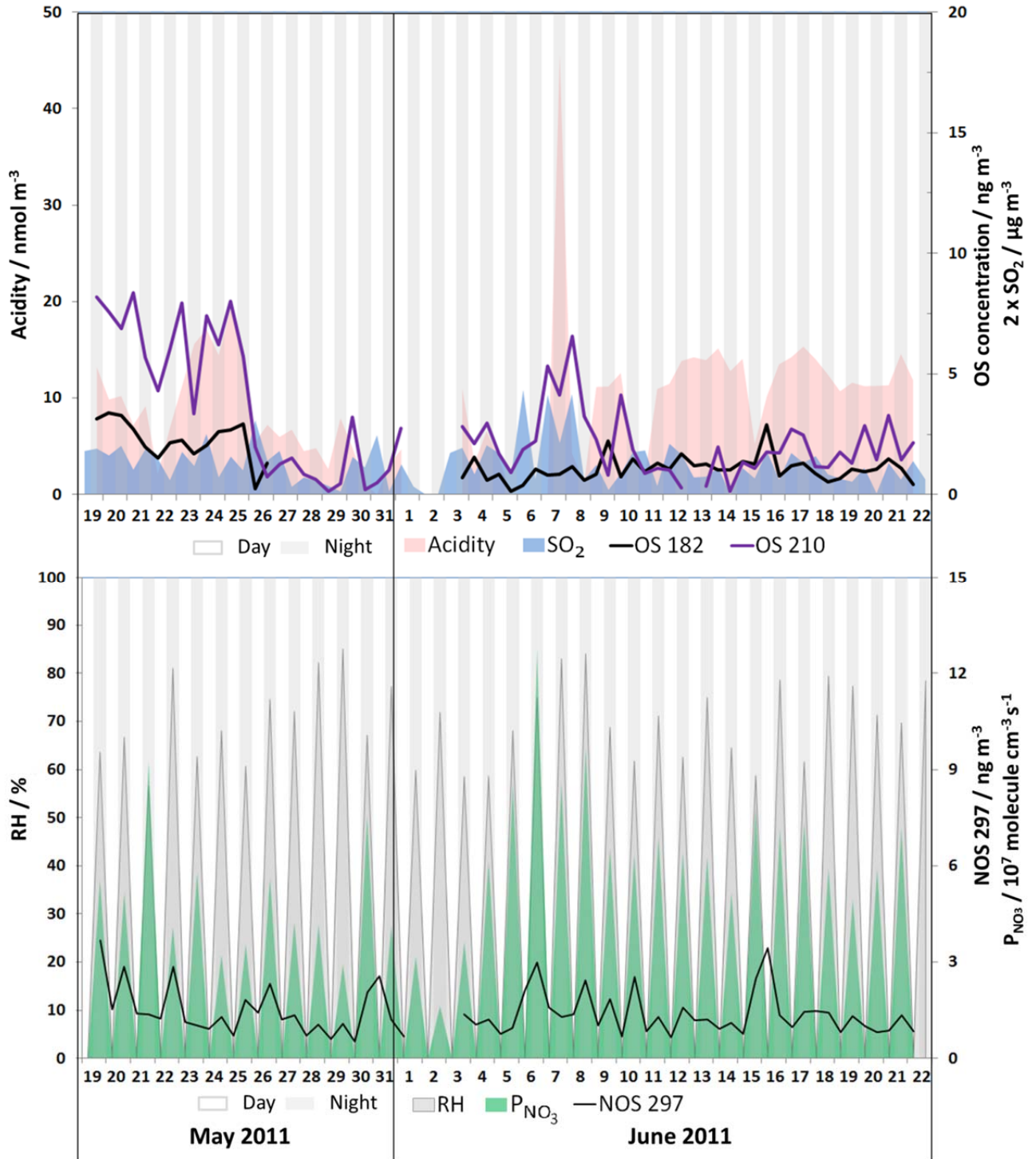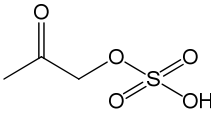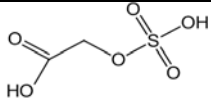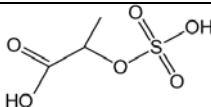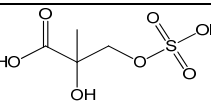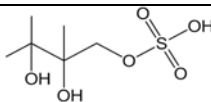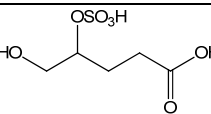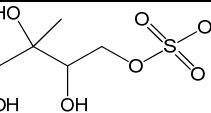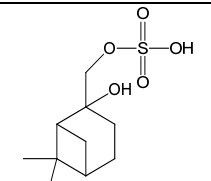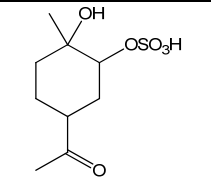
1 Table
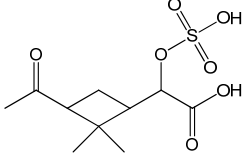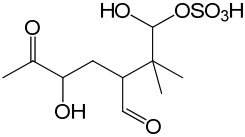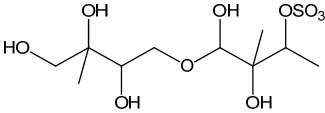
2 Table 1. Detected organic acids during the campaign. Related references on suggested precursors
3 are cited in the text.

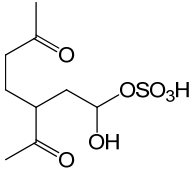| Organic acid	[M-H]$^-$ ion (m/z)	Retention time (min)	Proposed molecular formula	Proposed structure	Suggested precursors
Benzoic acid	121.022	27.5	$C_7H_6O_2$		Aromatic hydrocarbons
Adipic acid	145.058	14.9	$C_6H_{10}O_4$		Cyclic olefins
Pimelic acid	159.061	20.3	$C_7H_{12}O_4$		Cyclic olefins
Phthalic acid	165.123	19.0	$C_8H_6O_4$		Aromatic hydrocarbons
Terpenylic acid	171.058	18.3	$C_8H_{12}O_4$		α-pinene
Suberic acid	173.074	25.4	$C_8H_{14}O_4$		Fatty acids
Pinonic acid	183.100	27.5	$C_{10}H_{16}O_3$		α/β-pinene
Pinic acid	185.077	23.0; 24.0	$C_9H_{14}O_4$		α/β-pinene
Azelaic acid	187.091	28.1	$C_9H_{16}O_4$		Fatty acids
Hydroxy-pinonic acid	199.092	29.0	$C_{10}H_{16}O_4$		α/β-pinene
3-Methyl-1,2,3-butanetricarboxylic acid MBTCA	203.050	16.2	$C_8H_{12}O_6$		α/β-pinene

Di-terpenylic acid acetate (DTAA)	231.220	24.3	$C_{10}H_{16}O_6$		α-pinene

1

1 Table 2. Detected organosulfates (OS) during the campaign.
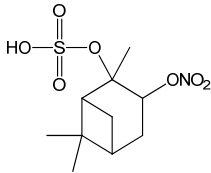
Organosulfate	[M-H]⁻ ion (m/z)	Retention time (min)	Proposed molecular formula	Proposed structure	Suggested precursors
OS 154[1,2]	152.981	3.6; 6.7	$C_3H_6O_5S$		hydroxyacetone (isoprene)
OS 156[3]	154.957	2.8	$C_2H_4O_6S$		glyoxal
OS 170[4]	169.047	3.4	$C_3H_6O_6S$		methylglyoxal
OS 182	181.063	34.8	$C_5H_{10}O_5S$	unknown	unknown
OS 200_1[1]	198.998	3.3	$C_4H_8O_7S$		2-methylglyceric acid (isoprene)*
OS 200_2[5,6]	199.001	3.4	$C_5H_{12}O_6S$		2-methyl-3-buten-2-ol (MBO)
OS 208	207.101	28.4; 29.5	$C_6H_8O_6S$	unknown	unknown
OS 210	209.086	28.0; 30.5	$C_7H_{14}O_5S$	unknown	unknown
OS 212[2]	210.983	4.8	$C_5H_8O_7S$	unknown	isoprene
OS 214[2,7,8]	213.001	3.5	$C_5H_{10}O_7S$	unknown	isoprene[2,5]
					fatty acid[4]
OS 216[1,2]	215.018	2.9	$C_5H_{12}O_7S$		2-methyltetrols (isoprene)**
OS 248[2]	247.061	32.2	$C_{10}H_{16}O_5S$	unknown	α-pinene
OS 250[2]	249.074	31.6	$C_{10}H_{18}O_5S$		β-pinene***
OS 252[2]	251.017	15.3	$C_9H_{16}O_6S$		limonene
OS 254[2]	253.158	21.3	$C_8H_{14}O_7S$	unknown	α-terpinene

OS 268[2]	267.225	19.7	$C_9H_{16}O_7S$		limonene
OS 280[2]	279.046	22.5; 25.2	$C_{10}H_{16}O_7S$		α/β-pinene
OS 298[2]	297.079	25.5	$C_{10}H_{18}O_8S$		α-pinene
OS 334[2]	333.071	38.0	$C_{10}H_{22}O_{10}S$		Isoprene

1 Included references were [1] Surratt et al. (2007a); [2] Surratt et al. (2008b); [3] Galloway et al. (2009); [4] Olson et al. (2011); ;
2 [5] Zhang et al. (2012c) [6] Zhang et al (2014) [7] Gómez-González et al., (2008); [8] Kristensen and Glasius, (2011). * OS 200
3 has been recently shown to specifically form from methacrylic acid epoxide (MAE) uptake onto acidified sulfate
4 aerosol (Lin et al., 2013). ** OS 216 has been shown to specifically derive from the reactive uptake of isoprene
5 epoxydiols (IEPOX) in the presence of acidic sulfate aerosol (Surratt et al., 2010; Lin et al., 2012). *** OS 250 can be
6 found in synthesis of both α and β-pinene derived organosulfates; however with different retention times. The OS 250
7 detected in this study was assigned to β-pinene precursor based on the corresponding retention time.

8

1   Table 3. Detected nitrooxy organosulfates (NOS) during the campaign.
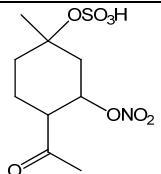
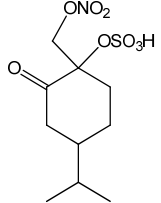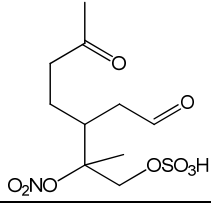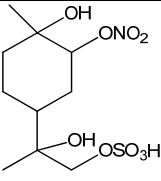| Nitrooxy organosulfate	[M-H]⁻ ion (m/z)	Retention time (min)	Proposed molecular formula	Proposed structure	Suggested precursors
NOS 295[2]	294.063	42.1; 44.7	$C_{10}H_{17}NO_7S$	More isomers	α/β-pinene
NOS 297[2]	296.063	32.8	$C_9H_{15}NO_8S$		limonene
NOS 311[2]	310.088	38.0	$C_{10}H_{17}NO_8S$		limonene, α-pinene
NOS 313[2]	312.209	28.0	$C_9H_{15}NO_9S$	unknown	limonene
NOS 327[2]	326.279	26.8	$C_{10}H_{17}NO_9S$		limonene, β-pinene, terpinolene
NOS 329[2]	327.994	33.5	$C_{10}H_{19}NO_9S$		limonene
NOS 331[2]	330.002	15.6	$C_9H_{17}NO_{10}S$	unknown	unknown
NOS 340[2]	339.070	25.7	$C_{10}H_{16}N_2O_9S$	unknown	α-pinene
NOS 343[2]	342.043	38.8	$C_{10}H_{17}NO_{10}S$	unknown	α-pinene; α-terpinene

2   References include [1] Surratt et al., (2007a); [2] Surratt et al., (2008b); [3] Surratt et al., (2010); [4] Gómez-González et al.,
3   (2008); [5] Kristensen and Glasius, (2011).

4

1   Table 4. Concentration range (ng m^{-3}) of the detected species at HCAB and Risø, reported as mean,
2   standard deviation (stdev.), median, max and the number of detected samples (N) at each site.

Compound	HCAB					Risø				
	Mean	Stdev.	Median	Max	N	Mean	Stdev.	Median	Max	N
Benzoic acid	0.4	0.6	0.1	2.0	14	1.4	1.9	0.4	7.2	26
Adipic acid	3.3	1.4	2.8	8.4	64	2.9	1.1	2.8	5.9	38
Pimelic acid	0.6	0.3	0.5	2.1	64	0.4	0.2	0.4	1.2	38
Phthalic acid	5.6	2.3	5.1	13.0	64	4.3	1.8	4.4	10.4	38
Terpenylic acid	1.6	1.6	1.1	8.9	64	1.4	1.7	0.9	8.5	38
Suberic acid	1.1	0.6	1.0	3.7	64	0.9	0.5	0.8	2.9	38
Pinonic acid	1.3	1.5	0.9	10.8	64	2.2	2.9	1.3	16.4	38
cis-Pinic acid	0.5	0.5	0.4	3.9	64	0.6	0.9	0.4	5.6	37
Azelaic acid	4.0	3.3	3.0	19.6	58	1.6	0.8	1.6	4.3	35
Hydroxy-pinonic acid	0.1	0.1	0.1	0.2	12	0.1	0.0	0.1	0.1	4
MBTCA	4.7	5.7	2.3	23.8	64	3.9	5.1	2.0	24.4	38
DTAA	0.4	0.5	0.2	2.0	64	0.2	0.3	0.1	1.4	34
Total organic acids	22.8	14.9	18.7	76.7	64	19.3	13.3	15.7	69.8	38
OS 154	6.6	6.0	4.5	25.7	63	5.3	4.6	4.3	24.6	38
OS 156	5.3	3.8	4.3	23.1	64	4.3	3.1	3.5	19.8	38
OS 170	3.5	2.3	2.7	10.3	63	3.1	2.0	2.5	11.5	37
OS 182	1.4	0.8	1.2	3.4	55	0.6	0.4	0.6	1.6	37
OS 200_1	7.1	6.7	4.4	33.1	64	4.5	3.9	3.0	22.2	37
OS 200_2	6.4	6.3	4.1	18.4	5	3.1	2.1	2.6	6.7	5
OS 208	5.0	3.3	5.7	14.2	63	4.1	0.8	4.1	5.6	38
OS 210	2.8	2.4	2.0	8.4	63	1.8	1.0	1.9	4.3	38
OS 212	7.4	6.0	5.0	32.2	64	6.2	4.7	4.6	27.8	38
OS 214	5.1	4.5	3.6	22.3	64	4.4	3.1	3.8	17.9	38
OS 216	5.0	6.8	2.8	36.9	60	3.2	3.3	2.4	20.8	34
OS 248	0.8	0.4	0.8	2.3	57	0.6	0.3	0.6	1.7	37
OS 250	2.3	1.1	2.1	6.8	64	2.4	2.1	1.9	12.4	38
OS 252	1.2	1.2	0.6	5.2	53	0.9	0.9	0.6	4.1	33
OS 254	1.3	1.5	0.8	7.9	63	1.1	1.2	0.8	7.4	38
OS 268	2.5	2.3	1.6	13.1	64	2.2	2.2	1.6	13.9	38
OS 280	2.6	2.5	1.8	11.5	60	2.2	2.0	1.6	10.3	38
OS 298	1.3	1.1	0.8	4.1	28	0.8	1.0	0.5	3.9	16
OS 334	0.6	0.3	0.6	1.0	8	0.8	-	0.8	0.8	1
Total organosulfates	59.8	44.5	43.8	130.6	64	46.9	31.1	36.3	144.0	38
NOS 295	0.5	0.6	0.3	4.2	46	0.4	0.3	0.4	1.2	15
NOS 297	1.4	0.7	1.3	3.7	64	0.9	0.6	0.7	3.4	38
NOS 311	0.9	0.8	0.4	2.4	7	0.5	0.5	0.4	1.8	8
NOS 313	0.7	0.7	0.5	3.4	56	0.6	0.6	0.5	3.0	30
NOS 327	0.9	0.7	0.7	3.6	48	0.6	0.6	0.5	2.8	29
NOS 329	0.8	0.9	0.4	3.6	19	0.5	0.6	0.3	2.6	17
NOS 331	0.3	0.2	0.2	1.2	41	0.3	0.3	0.2	1.5	26
NOS 340	0.2	0.1	0.2	0.2	3	-	-	-	-	-
NOS 343	0.8	0.4	0.8	1.4	24	0.4	0.4	0.4	1.0	4
Total nitrooxy organosulfates	3.9	1.3	2.8	3.7	64	2.8	1.2	2.1	1.8	36

3